1. Supporting Methods

1.1. Strains and general techniques for DNA manipulation.

For the construction of a disruption cassette and confirmation of the modified genotype, the genomic DNA isolated from *Chaetomium globosum* or CGKW14 or the transformants[1] was analyzed by PCR. Genomic DNA from above strains was prepared using the CTAB isolation buffer at pH 8.0 (20 g/L CTAB, 1.4 M sodium chloride and 20 mM EDTA). The gene-specific primers are listed in Table S1. PCR was performed using KOD Plus Neo (TOYOBO Co., Ltd.). Sequences of PCR products were confirmed through DNA sequencing (Macrogen Japan Corporation). *Escherichia coli* XL1-Blue (Stratagene) was used for plasmid propagation. DNA restriction enzymes were used as recommended by the manufacturer (Fermentas).

1.2. *In silico* analysis of genome sequence.

Protein sequences obtained by translating the *cgh* genes were used for BLASTP[2] query analyses performed against the NCBI GenBank database (http://www.ncbi.nlm.nih.gov) and the Broad Institute database (http://www.broadinstitute.org).

1.3. Spectroscopic analyses.

NMR spectra were obtained with a JEOL JNM-ECA 800 MHz spectrometer (^{1}H 800 MHz, ^{13}C 200 MHz), a JEOL JNM-ECA 600L MHz spectrometer (^{1}H 600 MHz, ^{13}C 150 MHz), a JEOL JNM-ECA 500 MHz spectrometer (^{1}H 500 MHz, ^{13}C 125 MHz) and a Bruker BioSpin AVANCE 400 MHz spectrometer (^{1}H 400 MHz, ^{13}C 100 MHz). ^{1}H NMR chemical shifts are reported in parts/million (ppm) using the proton resonance of residual solvent as reference: acetone-d_6 δ 2.05, pyridine-d_5 δ 7.19 and D_2O δ 4.79. ^{13}C NMR chemical shifts are reported relative to acetone-d_6 δ 29.84 and pyridine-d_5 δ 123.5.[3] Mass spectra were recorded with a Thermo SCIENTIFIC ACCELA Exactive liquid chromatography mass spectrometer by using both positive and negative ESI. LC–MS was conducted with a Thermo SCIENTIFIC ACCELA Exactive liquid chromatography mass spectrometer by using positive electrospray ionization. Samples were separated for analysis on an ACQUITY UPLC 1.8 μm, 2.1 x 50 mm C18 reversed-phase column (Waters) using a linear gradient of 5–100% (v/v) MeCN in H_2O supplemented with 0.05% (v/v) formic acid at a flow rate of 0.5 mL/min while the traces were monitored at 280 nm. Optical rotations were measured on a JASCO P-2200 digital

polarimeter. Infrared spectra were collected by an attenuated total reflectance with a JASCO FT/IR-4100.

1.4. Preparation of the deletion strains.

Deletion of target gene in *C. globosum* was carried out by homologous recombination using the *C. globosum* strain CGKW14 whose random nonhomologous recombination activity has been disabled by the disruptions of *CgligD* and *CgpyrG*.[4] A disruption cassette comprised of selection markers *pyrG* and *hph* flanked on both sides by a 1,000–1,500-base pair fragment that is homologous to the site of recombination in the *C. globosum* genome was introduced to CGKW14 to replace the target gene with the selection marker. Disruption of the target gene was confirmed by amplifying the disrupted segment from the genomic DNA by PCR.

1.5. Transformation and cultivation for production of secondary metabolites.

A mutant *C. globosum* strain was initially cultured on oatmeal agar plates at 30 °C for 14 days. Approximately 1×10^6 to 4×10^6 of sexual spores, or ascospores, collected from a single plate were used to inoculate 200 mL of MYG medium (10 g/L malt extract, 4 g/L glucose and 4 g/L yeast extract) containing 20 mM uridine and 0.18 mM uracil, which was shaken for additional 16 h at 30 °C. Grown cells were collected by centrifugation and washed with 1.0 M sorbitol. The cells were incubated with 4 mL of 1.0 M sorbitol containing 50 mg/mL lysing enzyme (Sigma-Aldrich) and 1,500 units of β-glucuronidase at room temperature for 3 h. The resulting protoplasts were filtered and subsequently centrifuged at 1,500 × *g* for 5 min at room temperature. The collected protoplasts were washed with 1.0 M sorbitol and centrifuged to remove the wash solution. The cells were suspended in 200 μL of STC buffer at pH 8.0 (1.0 M sorbitol, 10 mM calcium chloride and 10 mM Tris-HCl). Then 40 μL of PEG solution at pH 8.0 (400 mg/mL polyethylene glycol 8,000, 50 mM calcium chloride and 10 mM Tris-HCl) was added to the protoplast suspension. The mixture was subsequently combined with 4 μg of the DNA fragment with which the cells were to be transformed. The mixture was incubated on ice for 20 min to allow the transformation to proceed. After incubation on ice, 1 mL of the PEG solution was added to the reaction mixture, and the mixture was incubated at room temperature for additional 5 min. To select for hygromycin resistance, the DNA–protoplast mixture was plated initially on an MYG–sorbitol agar medium (MYG medium with 15 g/L agar and 1.0 M sorbitol) without marker antibiotics. After incubating the plate at 30 °C for 5 h, the cells were overlaid with an MYG–sorbitol agar

medium supplemented with 200 μg/mL hygromycin B to perform the selection. To prepare for a protoplast-mediated transformation of strains with *CgpyrG* deficiency, cells were plated on a RM–sorbitol agar plate (5 g/L glucose, 5 g/L potato starch, 2 g/L L-asparagine, 1.5 g/L ammonium chloride, 0.12 g/L magnesium sulfate, 1.4 g/L potassium phosphate monobasic, 1.5 g/L sodium phosphate dibasic, 0.3 g/L sodium sulfate, 1 mg/L thiamine-HCl, 15 g/L agar and 1.0 M sorbitol).[4] After 3 days of incubation at 30 °C, grown colonies were transferred onto a fresh MM (dextrose 10 g/L, L-asparagine 2 g/L, $MgSO_4 \cdot 7H_2O$ 0.2 g/L, NH_4Cl 1.5 g/L, KH_2PO_4 1.35 g/L, Na_2SO_4 0.3 g/L, Na_2HPO_4 1.45 g/L, thiamine-HCl 1 μg/mL and agar 15 g/L) or MYG containing hygromycin B agar medium and were incubated for several days at 30 °C. The resultant cells were transferred onto oatmeal agar plates and incubated for 3 days at 30 °C. The grown mycelia were inoculated into 20 mL of MYG liquid medium at 30 °C for 5 days shaken at 180 rpm. The broth was extracted with organic solvents for isolation of compounds. We carried out confirming the complementation of *cghA* and *C* by PCR using the chromosomal DNA isolated from the mutated strains of CGKW14 as a template by using the listed primer sets (Table S1).

1.6. Compounds purification and structural characterization.

To purify **1** (Figure 1 and Scheme 1) for structural analysis, CGKW14 (wild-type) was cultured in 4 × 1 L of MYG medium containing 20 mM uridine and 0.18 mM uracil, which was shaken at 30 °C for 7 days. After 7 days of incubation, the culture was centrifuged to separate the supernatant and the cells. The EtOAc extract was concentrated *in vacuo* to give an oily residue, which was then fractionated by silica gel flash column chromatography with $CHCl_3$/MeOH (1:0→0:1). The fraction eluted with $CHCl_3$/MeOH (4:1) was further purified by a reversed-phase HPLC (Wako Pure Chemical Industries, Ltd., Wakosil-II5 C18AR, 20 × 250 mm) on a linear gradient of 20 to 100% MeCN (v/v) in H_2O supplemented with 0.05% (v/v) trifluoroacetic acid (TFA) over 50 min and continuously 100% MeCN (v/v) in H_2O over 30 min at a flow rate of 8.0 mL/min at room temperature. To purify **7** (Scheme 1) for structural analysis, *ΔcghA*/CGKW14 was cultured in 12 × 1 L of MYG medium at 30 °C for 5 days. After 5 days of incubation, the culture was centrifuged to separate the supernatant and the cells. The supernatant was adjusted to pH 1.0 with $KHSO_4$. Subsequently, 12 liters of the supernatant was extracted with EtOAc (2 × 12 liters). The EtOAc extract was concentrated *in vacuo* to give an oily residue, which was then fractionated by ODS gel (Nacalai Tesque Inc., COSMOSIL 140 C_{18}-OPN) flash column chromatography with MeOH/H_2O (30/70→100/0)

with 0.05% (v/v) TFA. The sample was further purified by a reversed-phase HPLC (Nacalai Tesque Inc., COSMOSIL 5C18 MS-II, 20 × 250 mm) on an isocratic elution system of 70 % MeCN (v/v) in H_2O with 0.05% (v/v) TFA at a flow rate of 8.0 mL/min. Then the fraction was further purified by a reversed-phase HPLC (Nacalai Tesque Inc., CHOLESTER, 10 × 250 mm) on an isocratic elution system of 55 % MeCN (v/v) in H_2O with 0.05% (v/v) TFA at a flow rate of 4.0 mL/min to afford **7** (1.1 mg/L). Chemical structures of the isolated compounds **1** and **7** were identified from the spectroscopic data. The X-ray crystal structure of **1** was also determined as described below. Other biosynthetic products isolated in this study were purified using essentially the same experimental procedure as described above and their chemical structures were confirmed by HRESIMS and NMR.

1.7. Construction of disruption cassette and deletion strain from CGKW14.

To prepare a deletion strain of *C. globosum* missing a functional copy of a target *cgh* gene, initially a disruption cassette of each of the target gene was constructed. A disruption cassette included a selection marker (orotidine-5'-phosphate decarboxylase gene *CgpyrG* or hygromycin B phosphotransferase gene *hph*) flanked on both sides by a 1,000-base pair fragment that is homologous to the site of recombination at or near the ends of the target gene in the *C. globosum* genome. The disruption cassette was introduced into CGKW14 (*ΔCgpyrG/ΔCgligD*)[4] to allow homologous recombination to take place through which the target gene would be replaced by the selection marker. Disruption of the target gene was confirmed by amplifying the disrupted segment of the genomic DNA by PCR. For the construction of the disruption cassette, PCR was carried out using KOD Plus Neo DNA polymerase as recommended by the manufacturer. For the 1,000–1,500-base pair homologous region that is to be appended to each terminal of the selection marker (designated KO1 for 5' side-flanking fragment and KO2 for 3' side-flanking fragment as shown in Figure S1) to knock out the target gene via homologous recombination, both regions were amplified from the *C. globosum* genomic DNA by PCR. The following primer sets were used to prepare the required flanking homologous regions and selectable markers for each of the target genes:

Target gene	**Primer set for KO1**	**Primer set for *CgpyrG* or *hph***	**Primer set for KO2**
cghA	Cg02368_KO1_f1 Cg02368_KO1_r1	pyrG Fw pyrG Rv	Cg02368_KO2_f1 Cg02368_KO2_r1

cghB	Cg2369_KO_Fw1 Cg2369_KO_Rv1	hph_Fw hph_Rv	Cg2369_KO_Fw2 Cg2369_KO_Rv2
cghC	Cg02370_KO1_f1 Cg02370_KO1_r1	pyrG Fw pyrG Rv	Cg02370_KO2_f1 Cg02370_KO2_r1
cghD	Cg2371-ko-Fw1 Cg2371-ko-Rv1	hph_Fw hph_Rv	Cg2371-ko-Fw2 Cg2371-ko-Rv2
cghE	Cg2372-ko-Fw1 Cg2372-ko-Rv1	hph_Fw hph_Rv	Cg2372-ko-Fw2 Cg2372-ko-Rv2
cghF	9102-1Fw 9102-1Rv	pyrG Fw pyrG Rv	9102-2Fw 9102-2Rv
cghG	Cg02374_KO1_f1 Cg02374_KO1_r1	pyrG Fw pyrG Rv	Cg02374_KO2_f1 Cg02374_KO2_r1

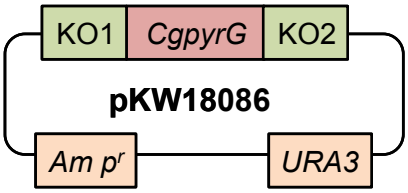

Figure S1. Map of plasmid pKW18086 carrying the disruption cassette for deleting *cghA* as a representative example of deletion plasmids prepared in this study. KO1: 1,500-bp 5'-side-flanking fragment homologous to one side of the recombination site in the CGKW14 genome; KO2: 1,500-bp 3'-side-flanking fragment homologous to the other side of the recombination site in the CGKW14 genome.

For the selection marker, either *CgpyrG* or *hph* was used. For preparing the disruption cassette for single mutant strains *ΔcghA*, *ΔcghC*, *ΔcghF* and *ΔcghG*, *CgpyrG* was used for selection. For preparing the disruption cassette for single mutant strains *ΔcghB*, *ΔcghD* and *ΔcghE*, *hph* was used. The *CgpyrG* gene encodes for an orotidine-5'-phosphate decarboxylase gene that allows both positive and negative selection. Positive selection can be performed in the presence of uridine and/or uracil and negative selection in the presence of 5-fluoroorotic acid. The *CgpyrG* gene was amplified from the genome DNA of *C. globosum* by PCR using the primer set of pyrG Fw/pyrG Rv. When *CgpyrG* was used as a selectable marker for the disruption, the transformants carrying the *CgpyrG* gene were selected on RM agar plates. The *hph* gene encodes for a hygromycin phosphotransferase that confers hygromycin resistance. It was amplified from pKW3202[6] by PCR using the primer set of hph_Fw/hph_Rv. When *hph* was used as a selectable marker for disruption, the selection medium was supplemented

with hygromycin B at a concentration of 200 μg/mL to select for transformants carrying the *hph* gene.

Amplified DNA fragments were visualized by agarose gel electrophoresis with ethidium bromide using UV (365 nm) transilluminator and purified with QIAquick Gel Extraction Kit (QIAGEN). Three purified fragments (KO1, KO2 and the selectable marker), each at 50 to 150 ng in a total volume of 45 μL, were mixed with the delivery vector pKW1250[7] (2 μg) pre-digested with *Sma* I (10 units) or pRS426[9] (2 μg) pre-digested with *Sac* I (10 units) and *Kpn* I (10 units) at 37 °C for 30 min. The mixture was transformed into *Saccharomyces cerevisiae* BY4741 for *in vivo* homologous recombination. These four DNA fragments were joined *in situ* by the endogenous homologous recombination activity of *S. cerevisiae* through the 25-bp homologous sequences present at the ends of those DNA fragments. The desired transformants were selected for the presence of the selection marker *URA3* on a uracil-deficient plate. The resulting plasmid (Figure S1) carrying the selection marker gene flanked by two 1,500 bp homologous regions was recovered from the yeast transformant and transferred to *E. coli*. The plasmid was amplified in *E. coli* for subsequent characterization by restriction enzyme digestion and DNA sequencing to confirm its identity. The PCR products were transformed into CGKW14. Transformants whose target gene was replaced by *CgpyrG* were selected on MM agar plates. Transformants whose target gene was replaced by *hph* were selected on MYG agar plates supplemented with 20 mM uridine, 0.18 mM uracil and 200 μg/mL hygromycin B. The selection confirmed the integration of the disruption cassette into the genome of the transformant.

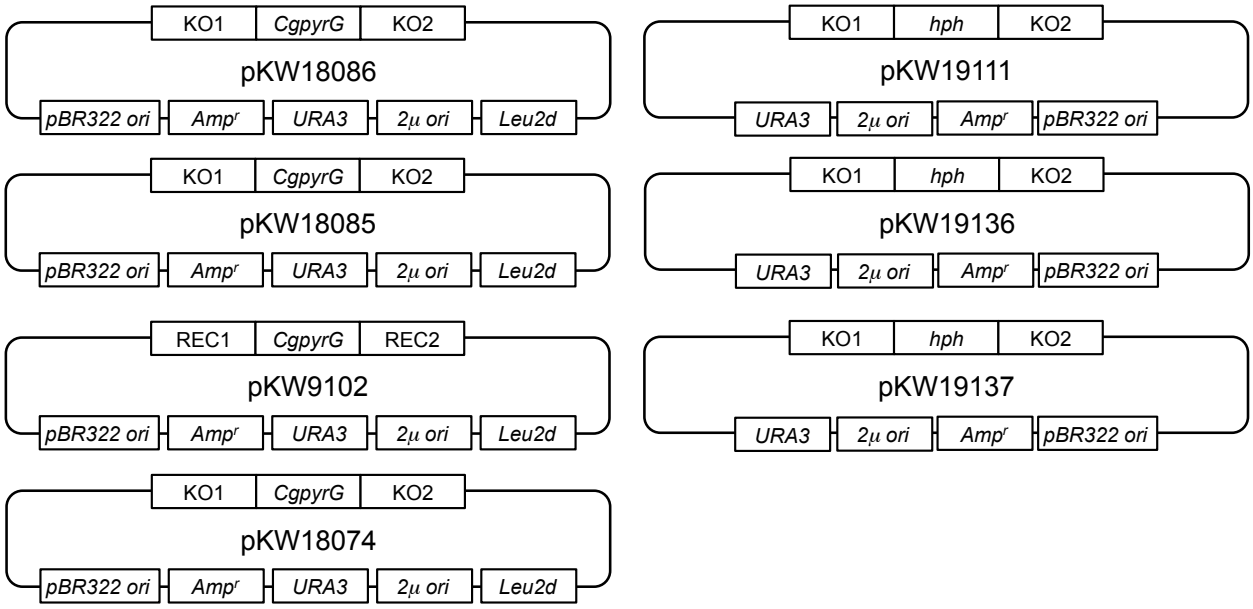

Figure S2. Map of plasmids for making the deletion mutants. pKW18086 for *cghA*; pKW19111 for *cghB*; pKW18085 for *cghC*; pKW19136 for *cghD*; pKW19137 for *cghE*; pKW9102 for *cghF*; pKW18074 for *cghG*. KO1: 1,000–1,500-bp 5'-side-flanking fragment homologous to one side of the recombination site in the CGKW14 genome; KO2: 1000~1500-bp 3'-side-flanking fragment homologous to the other side of the recombination site in the CGKW14 genome.

1.8. Confirmation of targeted deletion for *cghA*, *B*, *C*, *D*, *E*, *F* and *G* genes by PCR.

To verify that the cassette was inserted into the target gene, the genomic DNA isolated from the transformants was analyzed by PCR. Two sets of PCR primers were designed for this verification (Figure S3). For the first set, one primer that anneals at the 5' side of the KO1 region and another primer that anneals to the selection marker were designed. For the second primer set, one primer that anneals to the selection marker and another primer that anneals at the 3' side of the KO2 region were designed. With these primer sets, wild type genomic DNA will not produce any PCR product with this primer set. However, a PCR product will be formed from the genomic DNA of a strain containing desired gene deletion. Combination of the results from those two separate PCR reactions (Figure S4) ensured us that we had the targeted gene replaced by our desired selection marker.

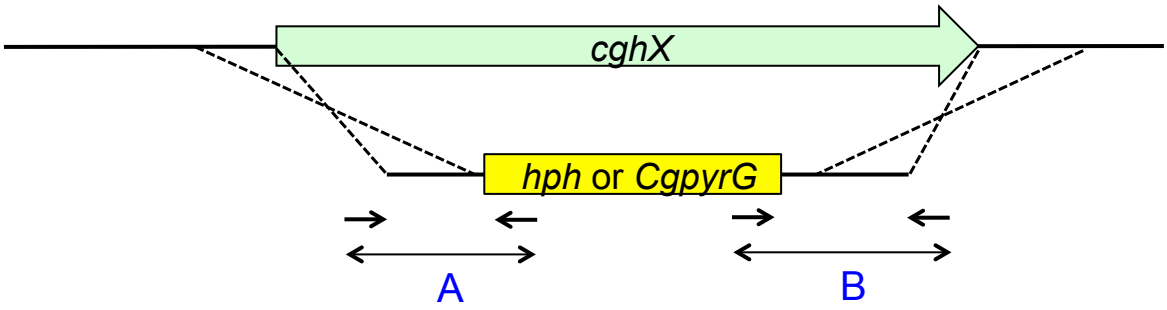

Figure S3. Detection strategy for the deletion strains by using PCR. Deficiency of the target genes by *CgpyrG* or *hph* as a selectable marker. A: left border of the marker region; B: right border of the marker region. *cghX*: *cghA*, *B*, *C*, *D*, *E*, *F* or *G*. Following are primer sets used for each of the deletion strains, where sequence of those primers are given in Table S1:

Deletion strain	PCR fragment	Forward primer	Reverse primer
ΔcghA	A	Cg2368_KO_Fw1	CgpyrG-Rv (*CgpyrG*)
	B	CgpyrG-Fw	Cg2368_KO_Rv1
ΔcghB	A	2369-KO-Fw	Cg-KO-hph-Rv (*hph*)
	B	Cg-KO-hph-Fw	2369-KO-Rv
ΔcghC	A	Cg2370_KO_Fw1	CgpyrG-Rv (*CgpyrG*)
	B	CgpyrG-Fw	Cg2370_KO_Rv1
ΔcghD	A	19136-Fw1	Cg-KO-hph-Rv (*hph*)
	B	Cg-KO-hph-Fw	19136-Rv1
ΔcghE	A	19137-Fw1	Cg-KO-hph-Rv (*hph*)
	B	Cg-KO-hph-Fw	19137-Rv1
ΔcghF	A	Cg2373-Fw2	CgpyrG-Rv (*CgpyrG*)
	B	CgpyrG-Fw	Cg2373_KO_Rv1
ΔcghG	A	Cg2374-Fw2	CgpyrG-Rv (*CgpyrG*)
	B	CgpyrG-Fw	Cg2374_KO_Rv1

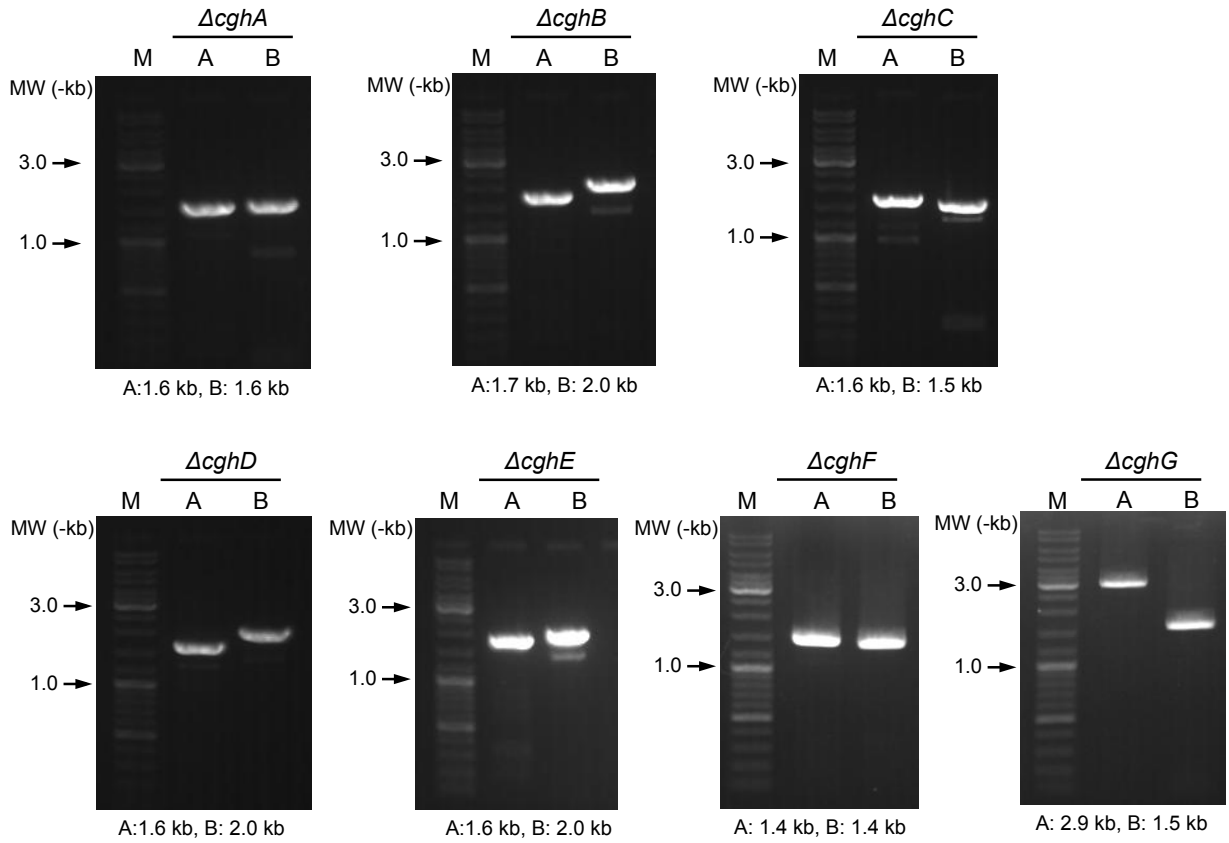

Figure S4. PCR analysis for confirming the deletion of *cghA*, *B*, *C*, *D*, *E*, *F* and *G* using the genomic DNA of each deletion strain as a template. M, molecular marker; Lane A, PCR fragment A; Lane B, PCR fragment B. Expected DNA size were shown below the pictures.

1.9. Complementation experiments for *cghA* and *C*, and confirming the production of **1**.

For the complementation of *cghA* and *C*, we began by constructing the vector for integrating *cghA* and *C* into the genome of *ΔcghA*/CGKW14 and *ΔcghC*/CGKW14, respectively. We chose the chaetoviridin biosynthetic PKS gene *cazM*[8] as the integration site so that complemented strains could be detected by the loss of production of chaetoviridins. Both 5' side-and 3' side-flanking fragments of *cazM* as shown in Figure S5, S6 were amplified by PCR using the 19133-Fw1/19133-Rv1 primer pair and the 19133-Fw3/19133-Rv3 primer pair, respectively (Table S1). In addition, two more DNA fragments, *hph* gene and *cghC* were amplified by PCR using the hph_Fw/hph_Rv and 19133-Fw2/19133-Rv2 primer sets (Table S1). These four DNA fragments were cloned into pRS426[9] linearized by restriction digestion with *Sac* I (10 units) and *Kpn* I (10 units) following the *in situ* homologous recombination method described above to yield pKW19133 (Figure S7). Similarly, the DNA fragment containing *cazM* of both 5' side-flanking fragment and 3' side-flanking fragment,

hph gene actin promoter[6] and *cghA* was amplified by PCR using the 19133-Fw1/19133-Rv1, 19138-Fw2/19133-Rv3, hph_Fw/19113-Rv2 and 19139-Fw1/19138-Rv1 primer sets (Table S1) and ligated with pRS426 that was digested with *Sac* I (10 units) and *Kpn* I (10 units) to yield pKW19139 (Figure S7). The plasmid was amplified in *E. coli* for subsequent characterization by restriction enzyme digestion and DNA sequencing to confirm its identity. The entire gene described in Figure S5 was amplified from pKW19133 using primer set 19133-Fw4/19133-Rv4 by PCR and integrated into a locus of *cazM* in the *C. globosum* genome because of no effect on secondary metabolites expect for chaetoviridin productions observed in our previous report.[4] Similarly, The entire gene described in Figure S6 was amplified from pKW19139 using primer set 19133-Fw4/19133-Rv4 by PCR and integrated into a locus of *cazM* in the *C. globosum* genome. The integration event was confirmed (Figure S9) following the strategy described in Figure S8.

For comparing the metabolic profiles of the strains with and without the complementation by HPLC analysis, we required the knock-out strain *ΔcazM*/CGKW14 as an experimental wild-type strain in this examination. We constructed a knock out cassette of the DNA fragments from the CGKW14 genome by PCR using primer sets chgg_07645_ko_Fw1/chgg_07645_ko_Rv1 and chgg_07645_ko_Fw3/chgg_07645_ko_Rv3 obtaining designated KO1 for 5' side-flanking fragment of *cazM* and KO2 for 3' side-flanking fragment of *cazM*, respectively. The *hph* gene was amplified from pKW3202 by PCR using hph_Fw/hph_Rv primer set (Table S1). These three DNA fragments were connected into one fragment by overlapping PCR. Again, the integration event was confirmed (Figure S9) following the strategy described in Figure S8.

The role of CghA and CghC in the selective formation of **1** in *C. globosum* was confirmed by complementing the *cghA*- and the *cghC*-disruption mutant with a functional copy of the *cghA* and the *cghC* gene, respectively (see Figure 4, iii vs. iv for *cghA* and Figure S14, iv vs. ix for *cghC*).

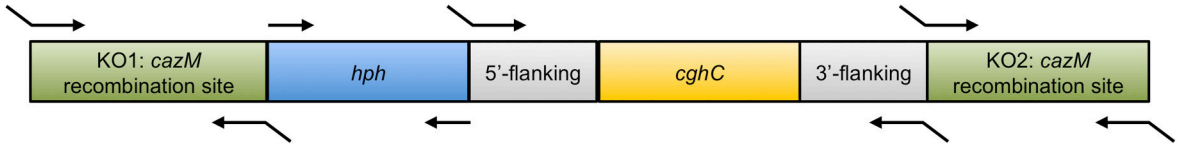

Figure S5. DNA fragment of the complementation experiments for *cghC* integrated into the locus of *cazM*.

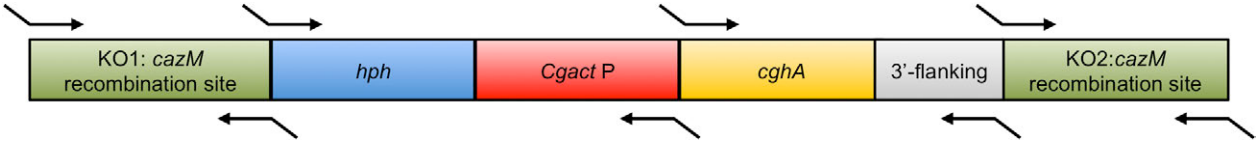

Figure S6. DNA fragment of the complementation experiments for *cghA* integrated into the locus of *cazM*. *Cgact* P: actin promoter isolated from *C. globosum*.[6]

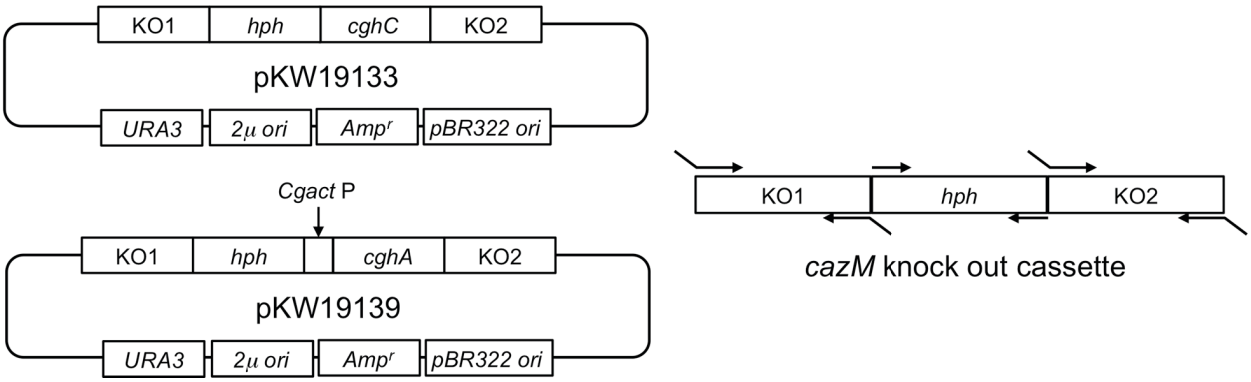

Figure S7. Map of plasmids for the complementation of *cghD* and *A*, and DNA fragment for preparing the mutant strain *ΔcazM*/CGKW14 as a wild-type of the complementation experiments. KO1: 1000-bp 5'-side-flanking fragment homologous to one side of the recombination site in the CGKW14 genome; KO2: 1000-bp 3'-side-flanking fragment homologous to the other side of the recombination site in the CGKW14 genome.

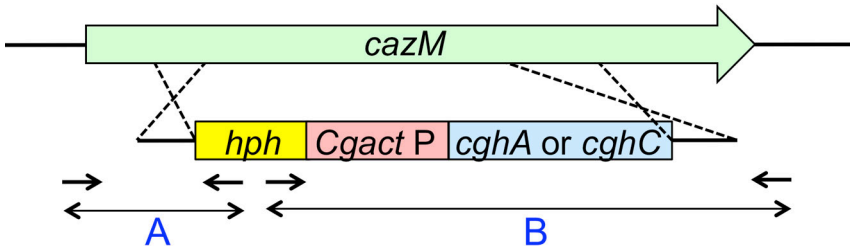

Figure S8. Detection strategy for confirming the complementation of *ΔcghA*/CGKW14 and *ΔcghA*/CGKW14 mutants by using PCR. *cazM* is replaced by a selectable marker *hph* and *cghA* or *cghC* with *Cgact* P into the genome of deletion strain, *ΔcghA*/CGKW14 or *ΔcghA*/CGKW14. A: left border of the marker region; B: right border of the marker region. *Cgact* P: actin promoter isolated from *C. globosum*. Following are primer sets used for each of the complementation strains, where sequence of those primers are given in Table S1:

Deletion strain	PCR fragment	Forward primer	Reverse primer
ΔcazM	A	19133-Fw5	Cg-KO-hph-Rv (*hph*)
	B	Cg-KO-hph-Fw	19133-Rv5
ΔcghA	A	19133-Fw5	Cg-KO-hph-R (*hph*)
	B	Cg-KO-hph-Fw	19133-Rv5
ΔcghC	A	19133-Fw5	Cg-KO-hph-Rv (*hph*)
	B	Cg-KO-hph-Fw	19133-Rv5

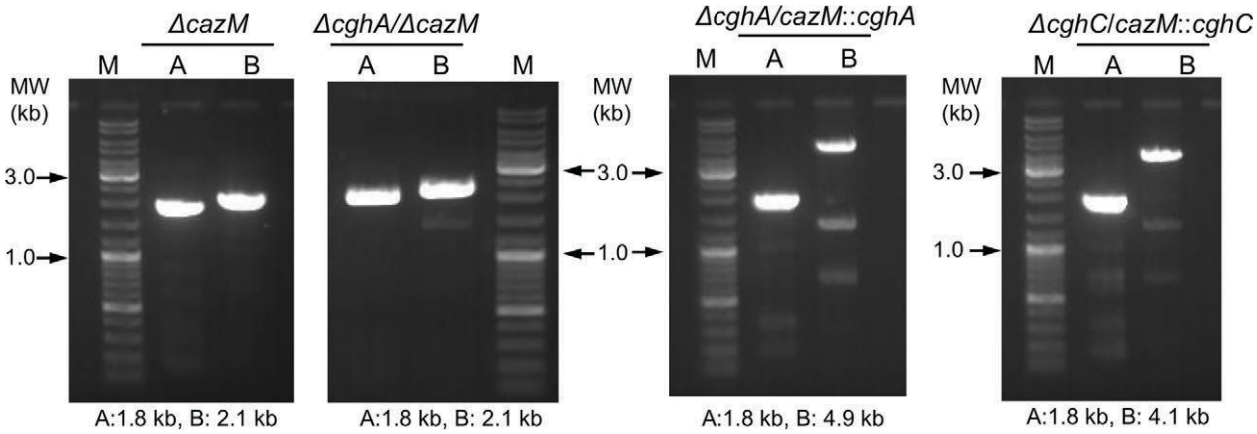

Figure S9. PCR analysis for confirming the complementation of *ΔcghA/cazM*::*cghA* and *ΔcghC/cazM*::*cghC* using the genomic DNA of each mutant as a template. PCR analyses of *ΔcazM* and *ΔcghA/ΔcazM* were employed as control results as well as metabolic profiles (Figure 4 in the main text). M, molecular marker; Lane A, PCR fragment A; Lane B, PCR fragment B. Expected DNA size were shown below the pictures.

1.10. Engineered biosynthesis of **1** and **7** by expression of *cghA*, *cghB*, *cghC* and *cghG* in *Aspergillus nidulans* A1145.

For molecular cloning of *cghG* from *C. globosum*, this strain was cultured in a CD medium for 7 days. The genomic DNA extraction was performed as described above. The *cghG* was amplified by PCR with four sets of primers pKW10027-f1/pKW10027-r4, pKW10027-f4/pKW10027-r5, pKW10027-f2/pKW10027-r2 and pKW10027-f3/pKW10027-r3 (Table S1) and combined with *Swa* I-digested (10 units) pKW20093[5] expression vector to generate pKW10027 (Figure S10) using yeast-based homologous recombination. The identity of the resulting vector pKW10027 was confirmed by DNA sequencing. This plasmid was used for expression of *cghG* for *in vivo* reactions.

The *AfpyroA* was amplified from of *A. fumigatus* A1159 genomic DNA[5] using the primer set pKW10011-f2/pKW10011-r2 (Table S1). The *p_amyB* was amplified from *A. niger* A1179 genomic DNA using the primer set pKW20118-f1/pKW20118-r1 (Table S1), *cghB* was amplified by PCR with a primer set pKW10029-f1/pKW10029-r1, *p_gpdA* was amplified from *A. niger* A1179 genomic DNA[5] using the primer set pKW10029-f2/pKW10029-r2 (Table S1), *cghC* was amplified by PCR with a primer set pKW10029-f3/pKW10029-r3 (Table S1), and pKW10029 was linearized by restriction digestion with *Swa* I (10 units). These DNA fragments were simultaneously introduced into *S. cerevisiae* BY4741 to combine them into an intact plasmid *in situ* by homologous recombination. The resulting plasmid was amplified in *E. coli* for restriction digestion analysis and later sequenced to confirm its identity. This plasmid was named pKW10029. This plasmid was used for expression of *cghB* and *cghC* for *in vivo* reactions.

The *cghA* was amplified by PCR with a primer set pKW10028-f1/pKW10035-r4 (Table S1), *AfriboB* was amplified from of *A. fumigatus* A1159 genomic DNA[5] using the primer set pKW10010-f1/pKW10010-r1 (Table S1) and combined with *Swa* I-digested (10 units) pKW20119[5] to generate pKW10035 (Figure S10) using yeast-based homologous recombination. The identity of the resulting vector pKW10035 was confirmed by DNA sequencing. This plasmid was used for expression of *cghA* for *in vivo* reactions.

Engineered biosynthesis of **1** and **7** was performed by using engineered *A. nidulans* A1145 that was transformed with pKW10027/pKW10029/pKW10035 or pKW10027/pKW10029 and grown with essentially the same procedure described in our report elsewhere.[28] Briefly, selected cells were grown overnight in CD-ST medium[28] at 30 °C for 48 hours with shaking at 180 rpm. The culture was transferred to 20 mL of the fresh CD-ST medium. Subsequently,

the culture was transferred to 4 L of the fresh CD-ST medium and incubated for an additional 144 hours at 30 °C. The analysis and purification of **1** and **7** were performed using essentially the same experimental procedure as described above, and their chemical structures were confirmed by HRESIMS and NMR. The results of the HPLC traces of metabolic extracts from engineered *A. nidulans* A1145 are given in **Figure 5** in the main text.

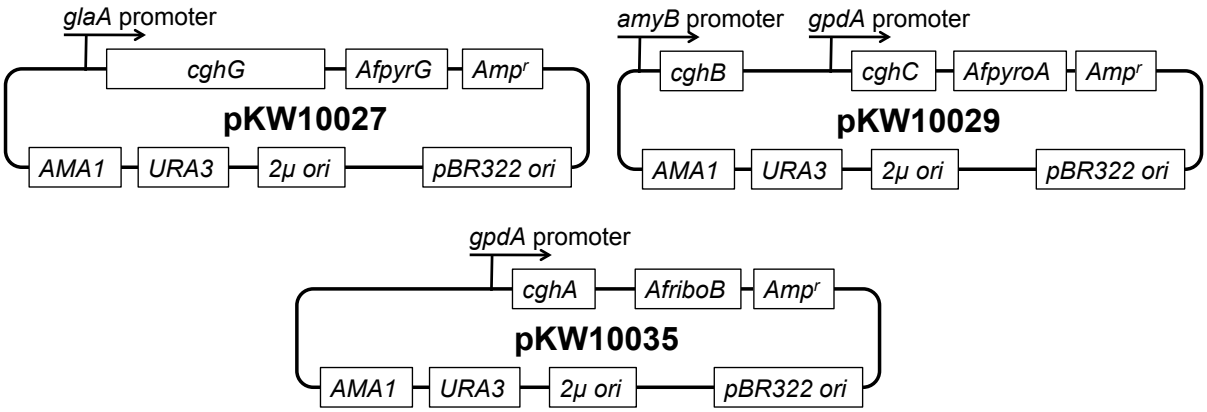

Figure S10. Map of plasmids for expression of *cghA*, *cghB*, *cghC* and *cghG* in *A. nidulans* A1145.

1.11. Bioconversion of **5** to **1** in *ΔcghB*/CGKW14.

CGKW14 was transformed with pKW19111 (Figure S2) for preparing the deletion mutant of *cghB*/CGKW14 by using selectable marker of a hygromycin phosphotransferase gene *hph*. Selected cells were grown overnight in MYG medium (20 mL) at 30 °C for 24 h with 180 rpm. The culture was transferred into 20 mL of the fresh MYG medium and the culture was incubated at 30 °C for 2 days. Substrate **5** was added to the medium to a final concentration of 1.4 mM, and the culture was incubated for an additional 5 days at 30 °C. The resultant culture was filtrated to separate the liquid medium and the cells. 1.0 mL of the liquid medium was extracted with ethyl acetate (2 × 1.0 mL). The ethyl acetate extract was combined and concentrated *in vacuo* to give an oily residue. The dried residue was dissolved in *N*,*N*-dimethylformamide (150 μL), and the resulting solution was subjected to LC–MS analysis. The LC–MS analysis was performed with a Thermo SCIENTIFIC Exactive liquid chromatography mass spectrometer using both positive and negative electrospray ionization. Samples were analyzed using an ACQUITY UPLC 1.8 μm, 2.1 × 50 mm C18 reversed-phase column (Waters) and separated on a linear gradient of 5–100% (v/v) MeCN in H_2O supplemented with 0.05% (v/v) formic acid at a flow rate of 500 μL/min. The results of the assay are given in Figure 5.

1.12. Construction of pKW19122 for expression of *cghB* in *E. coli.*

For expression of *cghB* in *E. coli*, *cghB* gene was amplified from cDNA that was synthesized from mRNA isolated from *C. globosum* with a primer set 19122-Fw1/19122-Rv1 (Table S1). The starting codon for *cghB* was reassigned from the annoted starting codon based on the sequence alignment between *cghB* and a homologous fungal aldolase CH063_07577 (Table 1 in the main text). A plasmid backbone was also amplified from pET28b vector with a primer set 19122-Fw1/19122-Rv1 (Table S1). These DNA fragments were then simultaneously joined together by using GeneArt Seamless Cloning and Assembly kit. The resulting plasmid was amplified in *E. coli* for restriction analysis with *Nco* I (10 units) and *Xho* I (10 units), and later sequenced to confirm its identity. This plasmid was named pKW19122 (Figure S11). This vector allowed production of CghB having a C-terminal His_6-tag. The plasmid carrying the correct copy of *cghB* was isolated from the *E. coli* transformant. The plasmid was amplified for restriction analysis and later sequenced to confirm its identity.

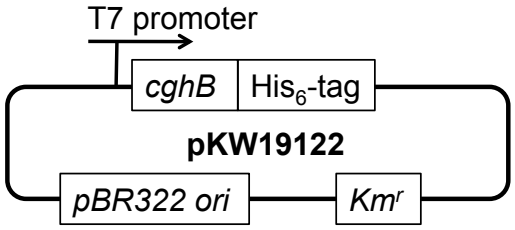

Figure S11. Map of plasmid pKW19122.

1.13. Protein production and purification of CghB.

Overexpression and subsequent protein purification of CghB was performed as follows: *E. coli* BL21 (DE3) harboring the plasmid pKW19122 was grown overnight in 20 mL of LB (lysogeny broth) with 50 μg/mL kanamycin at 37 °C. 3 liters of fresh LB with 50 μg/mL kanamycin was inoculated with 5 mL of the overnight culture and incubated at 37 °C until the optical density at 600 nm reached 0.6. Then expression of each gene was induced with 100 μM isopropylthio-β-D-galactoside at 18 °C. Incubation was continued for another 12 h, after which cells were harvested by centrifugation at 2,500 × *g*. All subsequent procedures were performed at 4 °C or on ice. Harvested cells were resuspended in disruption buffer (50 mM sodium phosphate buffer (pH 7.8), 300 mM NaCl). Cells were disrupted by French press (Ohtake Works, Co. Ltd.), and the lysate was clarified by centrifugation at 10,000 × *g*. The supernatant and the pellet were recovered as soluble and insoluble fractions, respectively.

The soluble fraction containing the protein of interest was applied to 3 mL of Ni-NTA Sepharose resin (GE Healthcare Life Sciences) previously equilibrated in the binding buffer, which is the disruption buffer supplemented with 20 mM imidazole. The column was washed with the binding buffer, then proteins were eluted with 10 mL of binding buffer supplemented with 250 mM of imidazole. Fractions containing proteins having the target molecular weight were pooled and dialyzed against 50 mM sodium phosphate buffer (pH 7.8), 50 mM NaCl, 1 mM $MgCl_2$. Protein concentration was estimated using the Bio-Rad protein assay kit (Bio-Rad Laboratories) with bovine immunoglobulin G as a standard. Purified protein samples were analyzed by SDS–PAGE using Tris-HCl gel stained with Coomassie Brilliant Blue R-250 staining solution (Figure S12). The purified protein was concentrated using a centrifugal filtration device (5 kDa molecular weight cutoff Amicon Ultra centrifugal unit, EMD Millipore Corp.), and was flash frozen in liquid nitrogen and stored at –80 °C until use for *in vitro* assays.

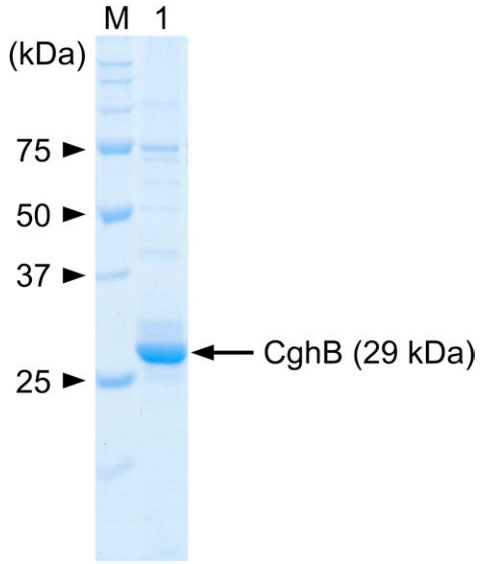

Figure S12. SDS–PAGE analysis of the purified CghB. Lane M: molecular weight marker; lane 2: CghB (29 kDa).

1.14. *In vitro* assay of CghB for elucidating the biosynthesis of **5**.

The assay mixture (20 mL) containing 50 mM of pyruvic acid, 10 mM cysteinesulfinic acid, 10 mM $MgCl_2$ was adjusted to pH7.5, and then CghB (1.4 μM) was added. After the mixture was incubated at 30 °C for 2 h, glutamic oxalacetic transaminase (50 units) was added and further incubated at 30 °C for 14 h. The products were purified through a 5 mL strong acidic resin column (Dowex 50Wx8, 100-200 mesh, H^+ form) and eluted with 15 mL of a 1 M NH_4OH solution. Crude products after evaporation were dissolved in 50% MeCN/H_2O (5

mL) followed by the addition of K_2CO_3 (0.29 mmol) and Fmoc-OSu (0.13 mmol). The reaction mixture was incubated at 0 °C for 1 h. The residue obtained after evaporation of the solvent was partitioned between EtOAc (5 mL × 3) and saturated $NaHCO_3$ solution (5 mL). The aqueous layer was acidified to pH 2.0 with 1N HCl and extracted with EtOAc (5 mL × 3). The extract was dried *in vacuo* and the residue was purified by C_{18} HPLC using a buffer comprised of 35:65 MeCN/H_2O containing 0.05% formic acid to give the Fmoc-protected (2*S*,4*S*)-4-hydroxy-4-methylglutamic acid **13**. Compound **13** was dissolved in *N*,*N*-dimethylformamide (600 µL) and deprotected by adding piperidine (300 µL). The reaction mixture was stirred at 25 °C for 2 h. After evaporation of the solvent, the residue was partitioned between EtOAc (5 mL × 3) and H_2O alkalified with 1N NH_4OH (5 mL). The aqueous layer was acidified with 1N formic acid, followed by application to a strong acidic resin and elution with 1 N NH_4OH. A pure sample of **5** was obtained and characterized by NMR.

Fmoc-protected (2*S*,4*S*)-4hydroxy-4-methyl glutamic acid **13**:
$[\alpha]_D^{23}$: –4.6 (*c* 0.17, MeOH); ^{1}H NMR (CD_3OD, 500 MHz): δ_H = 7.72 (2H, d, *J* = 6.8 Hz, Fmoc Ar CH), 7.60 (2H, t, *J* = 6.8 Hz, Fmoc Ar CH), 7.32 (2H, t, *J* = 6.8 Hz, Fmoc Ar CH), 7.25 (2H, t, *J* = 6.3 Hz, Fmoc Ar CH), 4.31-4.25 (3H, m, Fmoc CH or Fmoc CH_2), 4.16 (1H, t, *J* = 6.3 Hz, 2-CH), 2.35 (1H, m, 3-CH_2), 2.09 (1H, m, 3-CH_2), 1.39 (3H, s, 4-CH_3). ^{13}C NMR (CD_3OD, 125 MHz): δ_C = 179.0 (C5), 175.8 (C1), 158.2 [C(O)], 145.2 (Fmoc Ar quat C), 142.5 (Fmoc Ar quat C), 128.7 (Fmoc Ar CH), 128.2 (Fmoc Ar CH), 126.3 (Fmoc Ar CH), 120.9 (Fmoc Ar CH), 74.6 (C4), 68.2 (Fmoc CH_2), 52.4 (C2), 26.5 (4-CH_3);
ESI-MS: *m/z* 400 $(M+H)^+$; HRESIMS: *m/z* 400.1388 $(M+H)^+$, calcd. for $C_{21}H_{22}NO_7^+$, 400.1391, Δ = 0.3 mmu; IR (ATR) 1019, 1634, 1698, 2944, 3334 cm^{-1}.

5:
$[\alpha]_D^{20}$: –9.2 (*c* 0.25, H_2O); ^{1}H NMR (D_2O, 500 MHz): δ = 1.50 (s, 3H, CH_3), 2.05 (dd, 1H, *J* = 11.0, 15.0 Hz, part of CH_2), 2.56 (dd, *J* = 2.0, 15.0 Hz, part of CH_2), 3.71 (dd, 1H, *J* = 2.0, 11.0 Hz, CH); ^{13}C NMR (D2O, 125 MHz): δ = 29.5 (4-CH_3), 42.0 (C3), 56.2 (C2), 79.2 (C4), 177.0 (C1), 184.0 (C5);
ESI-MS: *m/z* 178 $(M+H)^+$; HRESIMS: *m/z* 178.0709 $[M+H]^+$, calcd. for $C_6H_{12}NO_5^+$, 178.0710, Δ = 0.1 mmu; IR (ATR) 1217, 1367, 1633, 1740, 3339 cm^{-1}.

1.15. Organic synthesis of substrate for (2*S*,4*S*)-4-hydroxy-4-methylglutamic acid **5** and (2*S*,4*R*)-4-hydroxy-4-methylglutamic acid **6**

Potassium 2-oxo-4-hydroxy-4-methylglutarate 14[10]:

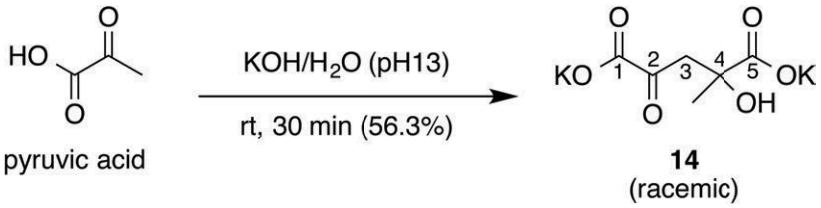

A solution of pyruvic acid (4 g, 45.4 mmol) in 50 mL of water was adjusted to pH 12 with a 6 N KOH solution. After 30 min of stirring, the pH is then adjusted to the neutrality by addition of a strong acidic ion exchange resin (Dowex 50WX8, 100 ± 200 mesh) and the resin removed by filtration. The keto acid is dissolved in a hydro-methanolic solution (MeOH/H_2O = 9/1) and then purified by two precipitations in diethyl ether to give a white solid yielding 3.2 g (56.3%), which was used for transamination without further purification.

(2*S*, 4*S*)-4-hydroxy-4-methylglutamic acid 5 and (2*S*, 4*R*)-4-hydroxy-4-methylglutamic acid 6[10]:

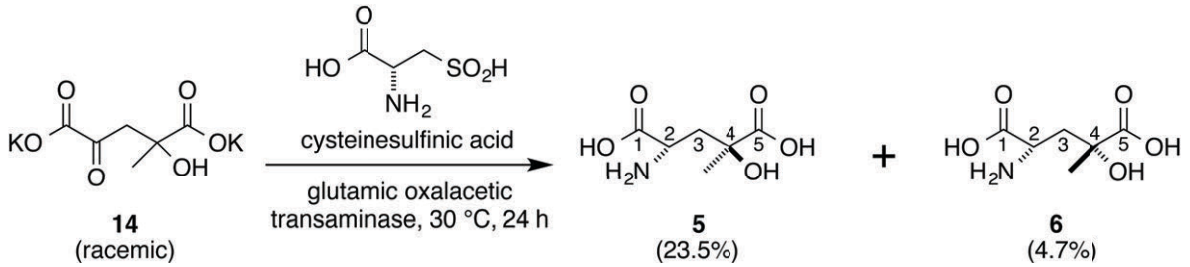

To a 1 mmol solution of the α-keto acid dilithium salt in 50 mL of distilled water was added 1.1 mmol of cysteinesulfinic acid monohydrate and the pH was adjusted to 7.5 by addition of a 1 M NaOH solution. Glutamic oxalacetic transaminase (100 units, Roche) was then added and the mixture was stirred during 24 h at 30 °C. The product was purified through a 10 mL strong acidic resin column (Dowex 50WX8, 100–200 mesh, H^+ form) and eluted with 20 mL of a 1 M NH_4OH solution. After evaporation of the alkaline solution, the mixture was applied to a column of a strong basic resin (Dowex 2X8, 200–400 mesh, 60 mL, acetate form). The column was eluted with 0.5 M acetic acid and fractionated. The column was washed with 40 mL of 0.5 M acetic acid. Compound **6** was initially eluted with 10 mL of 0.5 M acetic acid and then **5** was eluted with another 10 mL of 0.5 M acetic acid from the column. After the fractions containing amino acids **5** and **6** were evaporated separately, the each **5** and **6** was purified with application to a strong acidic resin and elution with 1 M NH_4OH.

6:

$[\alpha]_D^{20}$: –8.4 (*c* 0.31, H_2O); ^1H NMR (D_2O, 500 MHz): δ = 1.51 (s, 3H, CH_3), 2.15 (dd, 1H, *J* = 10.0, 15.0 Hz, part of CH_2), 2.39 (dd, *J* = 3.0, 15.0 Hz, part of CH_2), 4.00 (dd, 1H, *J* =3.0, 10.0 Hz, CH); ^{13}C NMR (D_2O, 125 MHz): δ = 27.1 (4-CH_3), 42.1 (C3), 54.6 (C2), 77.6 (C4), 177.4 (C1), 184.9 (C5);

ESI-MS: *m/z* 178 $(M+H)^+$; HRESIMS: *m/z* 178.0712 $[M+H]^+$, calcd. for $C_6H_{12}NO_5^+$, 178.0710, Δ = 0.2 mmu; IR (ATR) 1633, 3339 cm^{-1}.

Table S1. Oligonucleotide primer sequences. DNA primers were designed on the basis of sequence data obtained from the *C. globosum* and *Streptomyces hygroscopicus* (for *hph*) genome sequence database.

Primer name	Sequence
Cg02368_KO1_f1	5'- ATGGGTAAAAGATGTTAATTAACCCAAGTACCCATGCCGTGCTTGATTAC -3'
Cg02368_KO1_r1	5'- ACATCACCTCAAGTCAGCAGCGGCATTTCAGTTACTGTTGATGCTTTGGT -3'
Cg02368_KO2_f1	5'- CAAAAGGGAAGATCGCAGGTCAGGAAGGGTCACGCGCCTCAGTCTGAGTC -3'
Cg02368_KO2_r1	5'- CGCACACCACCACCACCACCACCCCTCTAATACGATAACCTTTTCACGTA -3'
Cg2369_KO_Fw1	5'- GGGCGAATTGGGTACAATCCCAAGGCGAGGGTTTTCTGTG -3'
Cg2369_KO_Rv1	5'- CAACAGGACTGTAGCTGGCGGCCAGCTGCACCACG -3'
Cg2369_KO_Fw2	5'- CTCCACCGTTCCATTATGGGTCTGGCGGGCATCTACAAC -3'
Cg2369_KO_Rv2	5'- GGGAACAAAAGCTGGAACCGGCATACTTCGGTAGCGGC-3'
Cg02370_KO1_f1	5'- ATGGGTAAAAGATGTTAATTAACCCGTACGTGTTCCTGGTGCGGTTGTAT -3'
Cg02370_KO1_r1	5'- ACATCACCTCAAGTCAGCAGCGGCACTTGAATTTGTTCTTGAGTTGTGTA -3'
Cg02370_KO2_f1	5'- CAAAAGGGAAGATCGCAGGTCAGGAGATGGGTATCTACCTGTAGGTGTGG -3'
Cg02370_KO2_r1	5'- CGCACACCACCACCACCACCACCCCCCACCGCTGATGCACAATCCACGGC -3'
Cg2371-ko-Fw1	5'- GGGCGAATTGGGTACGGGAGCTTCTATCCCGCCACGTTG -3'
Cg2371-ko-Rv1	5'- CAACAGGACTGTAGCACCTTGGCCCGCACGCAGCGTTCG -3'
Cg2371-ko-Fw2	5'- CTCCACCGTTCCATTGGTGGTTTGTATGAGTTGGGTCG -3'
Cg2371-ko-Rv2	5'- ACAAAAGCTGGAGCTGGATATCGGTCTAGTTATACGCACG -3'
Cg2372-ko-Fw1	5'- GGGCGAATTGGGTACGACCGAGGCAGTGGTGCTGAAGG -3'
Cg2372-ko-Rv1	5'- CAACAGGACTGTAGCGGGGCGGGACTCTGGGGAGGTCC -3'
Cg2372-ko-Fw2	5'- CTCCACCGTTCCATTTTACCATGAAGGTTGTGGCATTCTG -3'
Cg2372-ko-Rv2	5'- ACAAAAGCTGGAGCTCGGATCAGTTGGCGGCGATAATATTC -3'
9102-1Fw	5'- ATGGGTAAAAGATGTTAATTAACCCGCAGTGACCGCCGTACCAAATCCAC -3'
9102-1Rv	5'- ACATCACCTCAAGTCAGCAGCGGCATTTCCCGTGCTCGGCTGACTCAGG -3'
9102-2Fw	5'- CAAAAGGGAAGATCGCAGGTCAGGACGCTGGATGCAGTCGTCGCTGATGC -3'
9102-2Rv	5'- CGCACACCACCACCACCACCACCCCAAGCGCCATGAGGCTTCAGCTCGG -3'
Cg02374_KO1_f1	5'- ATGGGTAAAAGATGTTAATTAACCCCTGGTGCCCACGTACGCGGCGACGG -3'
Cg02374_KO1_r1	5'- ACATCACCTCAAGTCAGCAGCGGCAACGCCCAGGATCTTGGGGTCGGGCG -3'
Cg02374_KO2_f1	5'- CAAAAGGGAAGATCGCAGGTCAGGACGCATCCCCTACACGGGTCTGCTGG -3'
Cg02374_KO2_r1	5'- CGCACACCACCACCACCACCACCCCTGGTACCGGGCAATCAGGGAGCGGA -3'
chgg_07645_ko_Fw1	5'- ATGATTTCCGTAGCCGACCTCGATTATGCCTCCCGC -3'
chgg_07645_ko_Rv1	5'- GGCGCAACAGGACTGTAGCCGTTCTCGAGGATTTTCGGCGGGGTTGTATC -3'
chgg_07645_ko_Fw3	5'- GAACTTCTCCACCGTTCCATTCACCAAGATGAGCCACAACATCGCGGTGCGG -3'
chgg_07645_ko_Rv3	5'- TCAAAGGGCGTTTCCGTTGCCCGTTCCACGGGGG -3'
pyrG Fw	5'- TGCCGCTGCTGACTTGAGGTG -3'
pyrG Rv	5'- CTCCTGACCTGCGATCTTCCCT -3'
hph_Fw	5'- GCTACAGTCCTGTTGCGCCTTCCGG -3'
hph_Rv	5'- AATGGAACGGTGGAGAAGTTCCCTGGC -3'
Cg2368_KO_Fw1	5'- GTCGAAGGGGCACACCTCCATTTCC -3'
Cg2368_KO_Rv1	5'- GTGGATTTGCGAGTGAGTTGTGACAC -3'
2369-KO-Fw	5'- CGTGTCGCTGGACCCGTTTAGTG -3'
2369-KO-Rv	5'- GGGTACCGACCCCGTACGGAGTTG -3'
Cg2370_KO_Fw1	5'- GGTGGTGGTTTGTATGAGTTGGGTC -3'
Cg2370_KO_Rv1	5'- CTCCCTAGTTTAGCAACCGTGCTC -3'
19136-Fw1	5'- GACAAGCTTCAGTTCAGGGGTCCCT -3'
19136-Rv1	5'- GACCTGTGCGACTGGTTGTGCAATG -3'
19137-Fw1	5'- GATCGGGTAGTGATCAAAGCTCTG -3'
19137-Rv1	5'- GAGTCGGTAGAGTCGTCGTTAGTC -3'
Cg2373-Fw2	5'- GCAACCACGAGAATTCGAACAGACGTC -3'
Cg2373_KO_Rv1	5'- GGCATTTTCCATGTTTCCGGGTCG -3'
Cg2374-Fw2	5'- CTTCTAGCAGAAGGTCCATGACTGAAG -3'

Cg2374_KO_Rv1	5'- CACCGCCTCGAGAAGCTGGATGTCAG -3'
CgpyrG-Rv	5'- CCACAACATCACCTCAAGTCAGCAGC -3'
CgpyrG-Fw	5'- GAGCTCCAAAAGGGAAGATCGCAGG -3'
Cg-KO-hph-Rv	5'- GCACTCGTCCGAGGGCAAAGGAATAG -3'
Cg-KO-hph-Fw	5'- CGACAGACGTCGCGGTGAGTTCAG -3'
19133-FW1	5'- CTATAGGGCGAATTGGGTACATGATTTCCGTAGCCGACCTCGATTATG -3'
19133-Rv1	5'- CGCAACAGGACTGTAGCAGGATTTTCGGCGGGGTTGTATCTTGCTG -3'
19133-Fw2	5'- CTTCTCCACCGTTCCATTGGCTTCTCCCATAGTATTCCGCAGGC -3'
19133-Rv2	5'- CTCATCTTGGTGCCATTCTCATTTTACCGGGGAAATGGAGGTGTGC -3'
19133-Fw3	5'- GAGAATGGCACCAAGATGAGCCACAACATCGCGG -3'
19133-Rv3	5'- CTAAAGGGAACAAAAGCTGGTCAAAGGGCGTTTCCGTTGCCCG -3'
19133-Fw4	5'- GATTTCCGTAGCCGACCTCGATTATGCC -3'
19133-Rv4	5'- CAAAGGGCGTTTCCGTTGCCCG -3'
19113-Rv2	5'- CATTTTGACGGCTGGAAAGGTGC -3'
19138-Rv1	5'- GTGGCTCATCTTGGTGCGGCTTCTTGCCTCCGCAGCTGGG -3'
19139-Fw1	5'- CCAGCCGTCAAAATGGCGGCAGCTCCCTTCATTTC -3'
19138-Fw2	5'- CAAGAAGCCGCACCAAGATGAGCCACAAC -3'
19133-Fw5	5'- CCTGTGCGTTTCTTTCAACAGAATACC -3'
19133-Rv5	5'- GCACGAATGTCCAGTCCATCGAG -3'
19122-Fw1	5'- AAGAAGGAGATATACATGGCATCTTTCAACAATGTCTTGACCAAAG -3'
19122-Rv1	5'- TGGTGGTGGTGGTGCGAGTTTAGCAACCGTGCTCTATCAATC -3'
pKW10027-f1	5'- CAGCATCATTACACCTCAGCATTAATATGAGCGCCGCAGACCAGG -3'
pKW10027-r4	5'- CGATAGCATCCTCGTCACCAGACAGC -3'
pKW10027-f4	5'- GCTGTCTGGTGACGAGGATGCTATCG -3'
pKW10027-r5	5'- TGAGCGGGCGTCAGGCAC -3'
pKW10027-f2	5'- TCCCCGGCTGGTGGGGTAAC -3'
pKW10027-r2	5'- CAGTTCCGATCTCCAACGCCTTCTC -3'
pKW10027-f3	5'- GAGAAGGCGTTGGAGATCGGAACTG -3'
pKW10027-r3	5'- ACATACCCGTAATTTTCTGGGCATTTAAATCAACCCATCGGAAAAATAGCGGGAAA -3'
pKW20118-f1	5'- CGGGTGTTCTTGACGATGGCATCCTGCGGCCGCGATTAAAGGTGCCGAACGAG -3'
pKW20118-r1	5'- CGCCTACCGCAAGAGCCATCGCCATAAATGCCTTCTGTGGGGTTTAT -3'
pKW10029-f1	5'- ACAATAAACCCCACAGAAGGCATTTATGGCATCTTTCAACAATGTCTTGACCAAAG -3'
pKW10029-r1	5'- GGTCTCTCCCGTCACCCAAATCAATCCATCAGACGCAAGGAAGGGGAATA -3'
pKW10029-f2	5'- ATTCCCCTTCCTTGCGTCTGATGGATTGATTTGGGTGACGGGAGAGACC -3'
pKW10029-r2	5'- GGGTGGTGGCGGAAATAGCCATTGTTTAGATGTGTCTATGTGGCGGGGTAAT -3'
pKW10029-f3	5'- ATTACCCCGCCACATAGACACATCTAAACAATGGCTATTTCCGCCACCACCC -3'
pKW10029-r3	5'- AGACCCAACAACCATGATACCAGGGGATTTAAATCGTGTGAAGGGGATCAGAAAGTCTCG -3'
pKW10011-f2	5'- GTAGGATCAGTAGGAAAGCCAGGCTGCAATTTAAATCCCCTGGTATCATGGTTGTTGGGTCT -3'
pKW10011-r2	5'- AGACCCAACAACCATGATACCAGGGGATTTAAATTGCAGCCTGGCTTTCCTACTGATCCTAC -3'
pKW10028-f1	5'- CCCGCCACATAGACACATCTAAACAATGGCGGCAGCTCCCTTCATTT -3'
pKW10035-r4	5'- GGGTATCATCGAAAGGGAGTCATCCAATTTAAATAGTGTAACGTTTGCGTTTGCGGC -3'
pKW10010-f1	5'- GTCCAACAATCCGCGAAGTCGATCATTTAAATTGGATGACTCCCTTTCGATGATACCC -3'
pKW10010-r1	5'- TCCTTTTTCAATGGGCAATTGATTACGGAAATGACGCACTGCCACCACGATAG -3'

2. Supporting Results

2.1. Newly identified a biosynthetic gene cluster responsible for producing **1** in *C. globosum*.

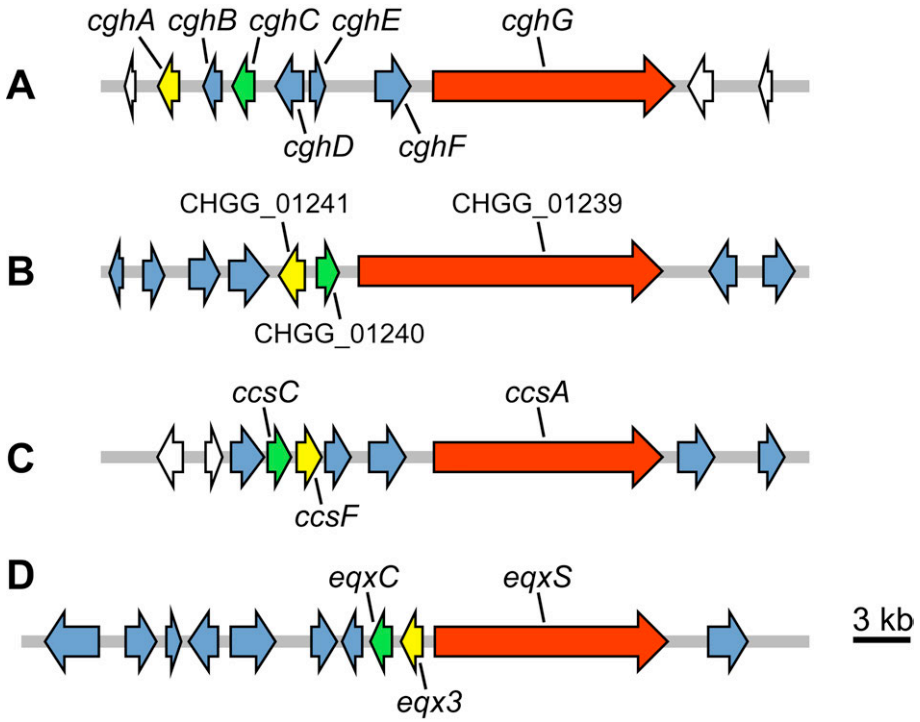

Figure S13. The *cgh* cluster and other gene clusters proposed to code for a Diels–Alderase in *C. globosum* (CHGG), *Aspergillus clavatus* (ccs) and *Fusarium heterosporum* (*eqx*). The overall organization of (A) Sch 210972, (B) chaetoglobosin A,[12] and (C) cytochalasin E[13] and (D) equisetin[14,15] biosynthetic gene clusters are shown. Predicted Diels–Alderase gene is colored in yellow, while the PKS–NRPS and its associated stand-alone enoylreductase genes are shown in red and green, respectively. Predicted function of the translation product of each of the gene found in the Sch 210972 gene cluster is given in **Table S2**.

Table S2. Deduced functions of the ORFs in the Sch 210972 biosynthetic gene cluster from *C. globosum*.

Locus ID	Gene name	Amino acids (no.)	Deduced function (homolog, NCBI accession number, species)	Identity/ Similarity (%)
CHGG_02368	*cghA*	396	hypothetical protein *ccsF* (*A. clavatus*, ACLA_78690)	25/37
CHGG_02369	*cghB*	270	HpcH/HpaI aldolase (*Colletotrichum higginsianum*, CH063_07577)	55/71
CHGG_02370	*cghC*	375	enoyl reductase *ccsC* (*A. clavatus*, ACLA_78700)	38/56
CHGG_02371	*cghD*	484	GAL4 transcription factor *eqxR* (*Fusarium heterosporum*)	27/40
CHGG_02372	*cghE*	137	hypothetical protein	–/–
CHGG_02373	*cghF*	528	fungal transcription factor *eqxF* (*F. heterosporum*)	29/40
CHGG_02374-8	*cghG*	3031	PKS–NRPS *ccsA* (*A. clavatus*, ACLA_078660)	45/61

Deduced function of the ORFs was determined based on the sequence similarity/identity to known proteins as determined by Protein BLAST (BLASTP) search[2] against the NCBI non-redundant database. N/A, no differentiation was observed from the culture of deletion mutant.

2.2. Deletion study of the Sch 210972 biosynthetic gene cluster.

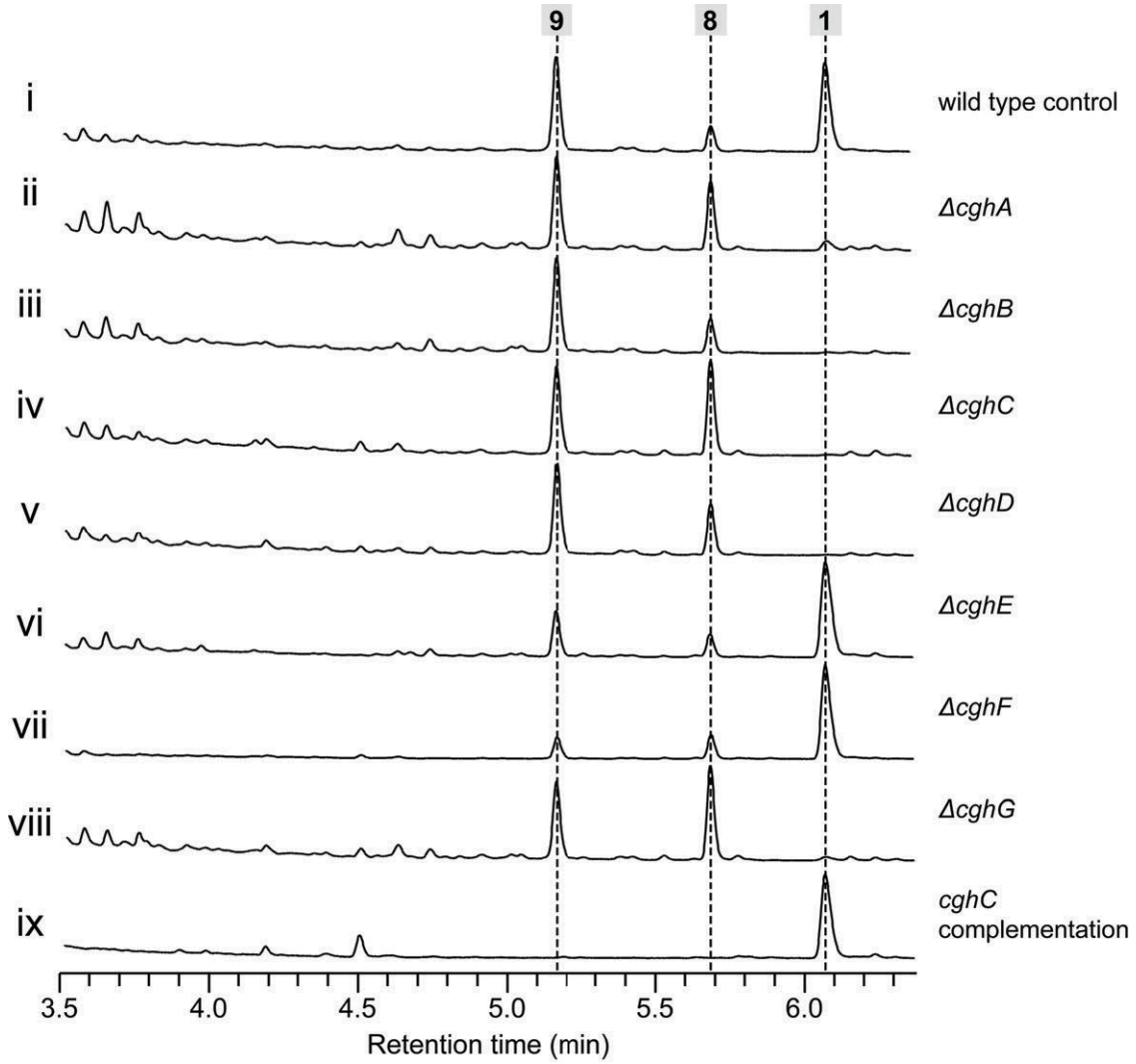

Figure S14. HPLC traces of metabolic extracts from the cultures of various *C. globosum* strains to identify the genes responsible for the biosynthetic steps involved in the formation of **1** during the Sch 210972 biosynthesis. All deletion strains were prepared in CGKW14 by replacement with *CgpyrG* or *hph* into the target gene via homologous recombination.[4] All cultures were grown in MYG medium. All HPLC traces were monitored at 290 nm. Extract of the culture of (i) CGKW14 as a wild-type control, (ii) *ΔcghA* strain, (iii) *ΔcghB* strain, (iv) *ΔcghC* strain, (v) *ΔcghD* strain, (vi) *ΔcghE* strain, (vii) *ΔcghF* strain, (viii) *ΔcghG* strain and (ix) *ΔcghC*/*cazM*::*cghC*/CGKW14 strain. **8**: chaetoviridin A; **9**: chaetoviridin B.[11]

2.3. Feeding experiments of **5** and **6** in *ΔcghB*/CGKW14.

The grown mycelia on an MYG–sorbitol agar medium were inoculated into 20 mL of MYG liquid medium supplemented with **5** or **6** at final concentration of 1.4 mM at 30 °C for 3 days shaken at 180 rpm. The resultant culture (1.0 mL) was terminated by extraction with ethyl acetate (2 × 1.0 mL). The extract was dried *in vacuo*. The dried residue was dissolved in DMF (150 μL), and the resulting solution was subjected to LC–MS analysis. The LC–MS analysis was performed with essentially the same procedure described above. *ΔcghB*/CGKW14 without supplemented **5** and **6** was used as a negative control.

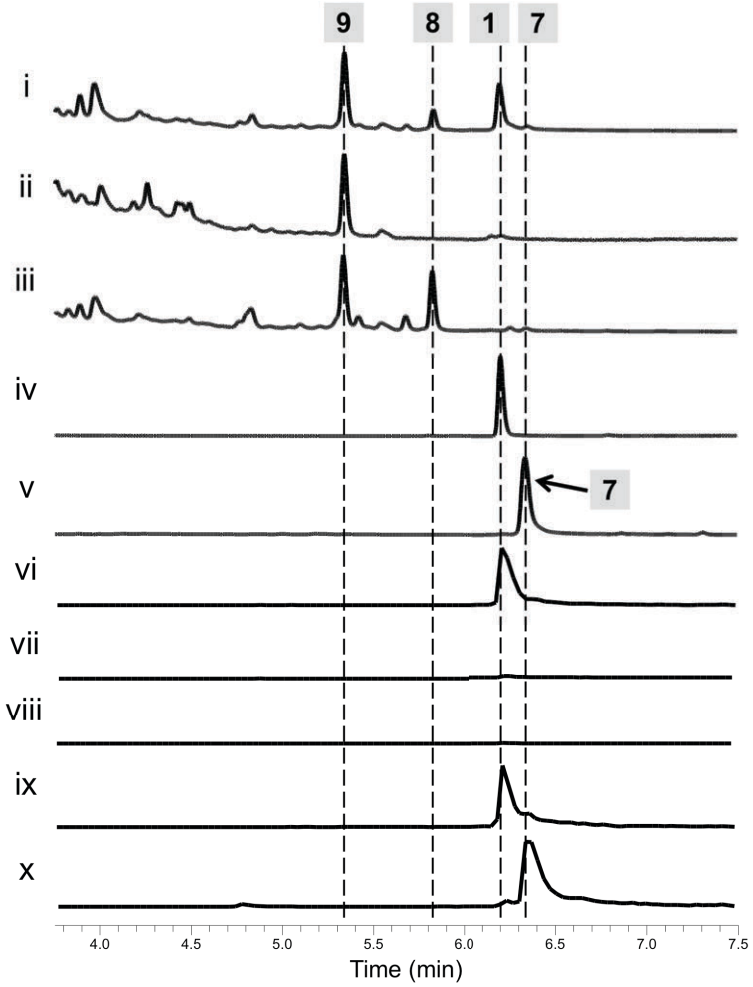

Figure S15. Feeding experiments of **5** and **6** in *ΔcghB*/CGKW14. UV trace of the reaction (i) in the presence of **5**, (ii) **6**, (iii) without feeding of **5** or **6** negative control, and authentic references of (iv) **1**, and (v) **7**. The UV traces were monitored at 280 nm. Extracted LC traces corresponding to the m/z^+ for **1** and **7** (m/z^+ = 446, vi–x). Extracted LC trace of the reaction (vi) in the presence of **5**, (vii) **6**, (viii) without feeding of **5** or **6** negative control, and authentic references of (ix) **1**, and (x) **7**. **8**: chaetoviridin A; **9**: chaetoviridin B.[11]

2.4. Chemical and structural characterization of **1**.

Table S3. NMR data of compound **1** in acetone-d_6. The molecular formula of **1** was established by mass data [ESI-MS: *m/z* 446 $(M+H)^+$; HRESIMS: *m/z* 446.2535 $(M+H)^+$, calcd. for $C_{25}H_{36}NO_6^+$, 446.2537, Δ = 0.17 mmu]; $[\alpha]_D^{25}$: +47.3 (*c* 0.24, acetone).

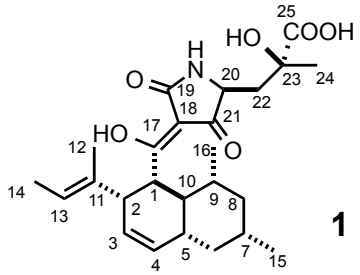

1

Position	δ_H [ppm] mult. (*J* in Hz)[11]	δ_H [ppm] mult. (*J* in Hz)	δ_C [ppm][11]	δ_C [ppm]
1	3.94 dd (8.0, 7.0)	3.93 dd (8.9, 7.9)	46.9	46.9
2	3.00 dt (8.0, 1.0, 1.0)	2.99 brd (7.9)	48.5	48.6
3	5.66 brs	5.67 brs	129.4	129.2
4	5.66 brs	5.67 brs	134.5	134.4
5	1.85 m	1.86 m	41.2	41.2
6a	1.91 m	1.91 m	42.6	42.3
6b	0.95 m	0.94 m		
7	1.63 m	1.63 m	33.2	33.2
8a	1.66 m	1.66 m	46.6	46.6
8b	0.83 m	0.83 m		
9	1.39 m	1.39 m	39.9	39.9
10	1.40 m	1.40 m	46.9	46.8
11			136.2	136.2
12	1.57 brs	1.57 brs	16.8	16.0
13	5.19 dq (6.5, 1.0)	5.19 brq (6.5)	122.3	122.3
14	1.50 brd (6.5)	1.50 brd (6.9)	13.8	13.7
15	0.91 d (6.5)	0.91 d (6.5)	22.6	22.6
16	0.85 d (6.5)	0.85 d (6.5)	21.4	21.4
17			194.9.	194.9
18			101.4	101.4
19			176.6	176.5
20	3.80 dd (10.0, 2.5)	3.79 dd (9.9, 2.5)	60.9	60.9
21			193.5	193.4
22a	2.50 dd (14.0, 2.5)	2.49 dd (14.4, 2.5)	42.7	42.6
22b	1.75 dd (14.0, 10.0)	1.74 dd (14.4, 9.9)		
23			75.1	75.1
24	1.49 s	1.49 s	27.7	27.8
25			177.2	177.6

^{1}H and ^{13}C NMR spectra were recorded at 500 MHz and 125 MHz, respectively.

Fig. S16. [1]H NMR of **1** in acetone-d_6 (500 MHz).

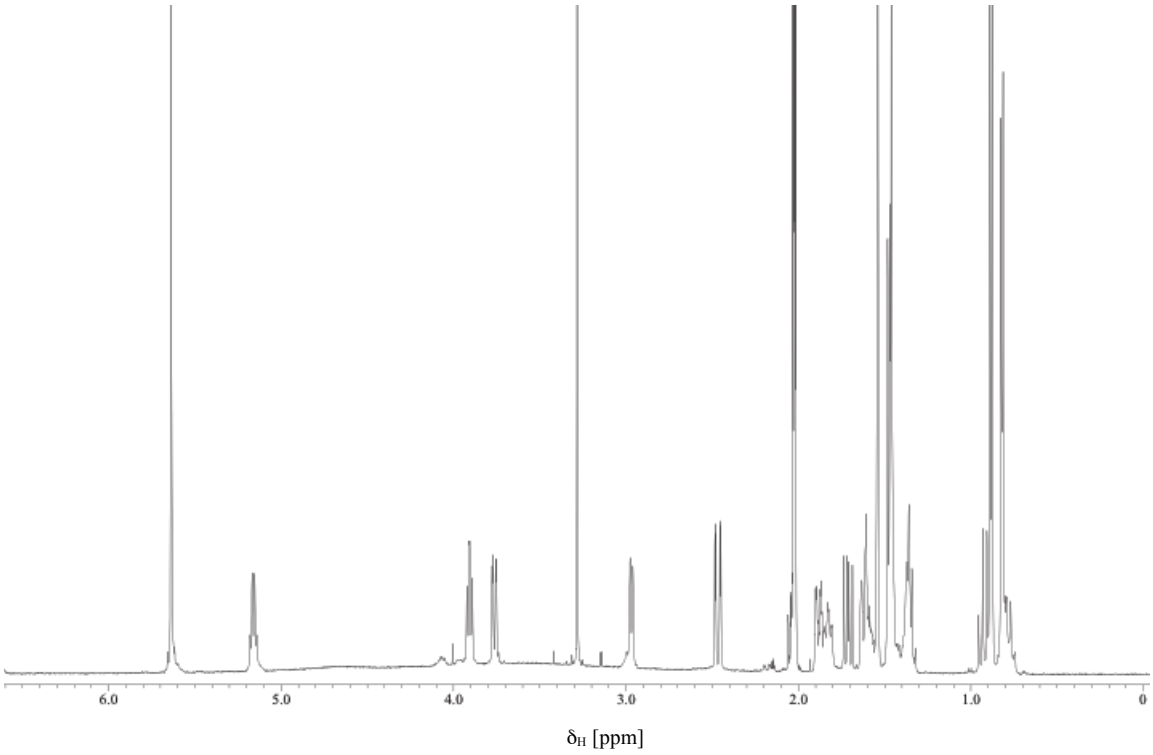

Fig. S17. [13]C NMR of **1** in acetone-d_6 (125 MHz).

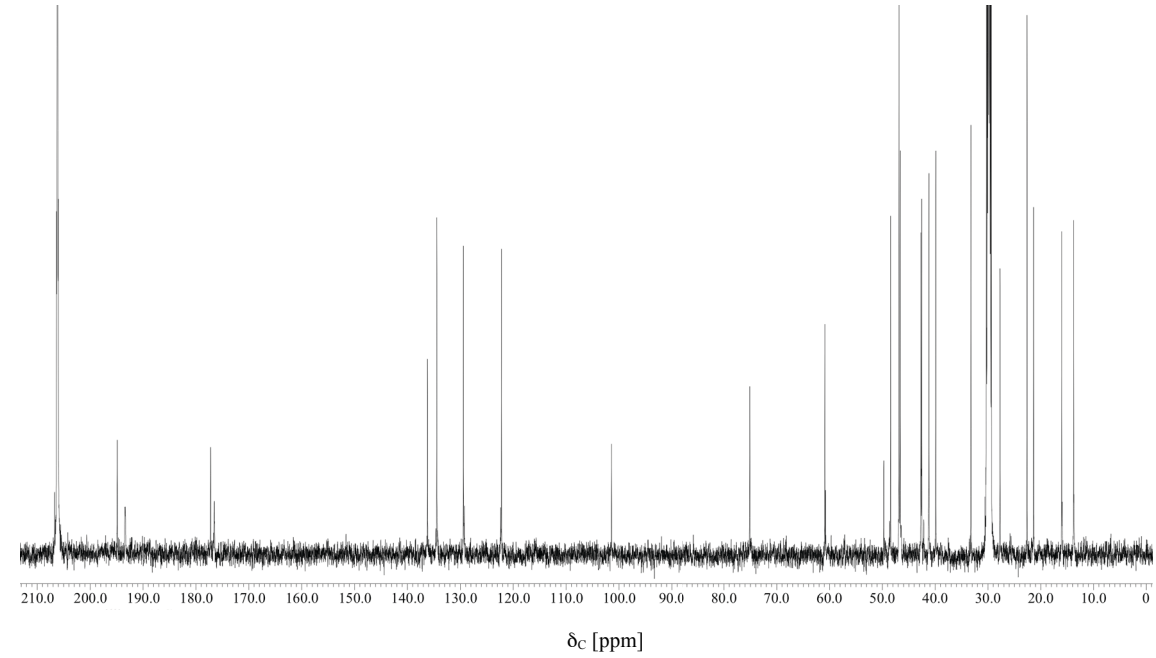

X-ray single crystal analysis of **1** for determination of absolute configuration. Colorless prismatic crystals were obtained from MeOH, mp 104–105°C; Crystal data of **1**: Monoclinic space group $P2_1$, a = 11.6604(4) Å, b = 6.2663(2) Å, c = 18.5264(6) Å, β = 93.2160(18)°, V = 1351.55(8) Å^3, Z = 2, ρ = 1.174 Mg/m^3, in the final least-squares refinement cycles on F_2, the model converged at R_1 = 0.0701, wR_2 = 0.2159, and GOF = 1.133 for 9784 reflections (Figure S18). The absolute configuration was determined as 1*R*, 2*S*, 5*R*, *7S*, 9*R*, 10*S*, and *20S*, 23*S* based on the data described in the CIF. Crystallographic data for **1** have been deposited at the Cambridge Crystallographic Data Center (deposition number CCDC 1012146).

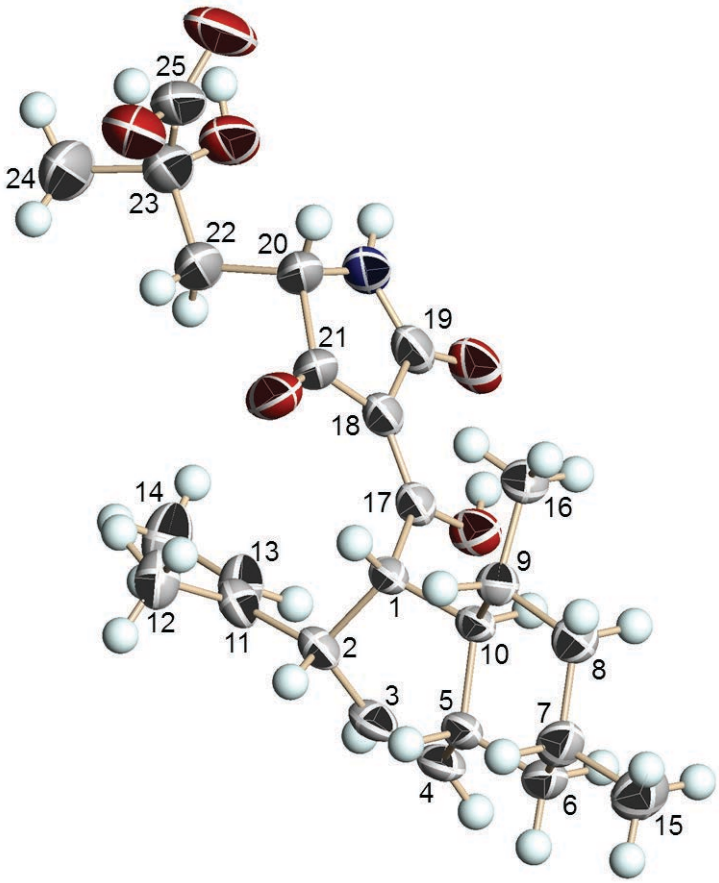

Figure S18. ORTEP representation of the crystal structure of **1**.

2.5. Chemical characterization of **7**.

Table S4. NMR data of compound **7** in pyridine-d_5. The molecular formula of was established by mass data [ESI-MS: *m/z* 446 $(M+H)^+$; HRESIMS: *m/z* 446.2538 $(M+H)^+$, calcd. for $C_{25}H_{36}NO_6^+$, 446.2537, Δ = 0.14 mmu]; $[\alpha]_D^{25}$: –72.0 (*c* 0.2, acetone).

Position	δ_H [ppm]		mult. (*J* in Hz)	HMBC	δ_C [ppm]
1	4.49	1H	brs	10,11,17	42.8
2	3.23	1H	brs	1,3,11,13,17	44.7
3	5.92	1H	d (10.1)	2,4,5	129.7
4	5.75	1H	m	3,5,10	133.5
5	2.63	1H	brs	6	33.2
6	1.69	1H	m	5	39.9
	1.13	1H	m	4	
7	1.55	1H	m	6,8	28.6
8	1.48	1H	m	7,9	44.2
	0.65	1H	m	7,9,10,15,16	
9	1.87	1H	m	10	31.7
10	1.85	1H	m	4	45.5
11					137.8
12	1.77	3H	s	11,13	15.7
13	5.43	1H	m	2,12	120.4
14	1.57	3H	m	11,12,13	14.0
15	0.80	3H	dd (11.9, 6.4)	6,7,8	23.1
16	1.23	3H	m	9,10	21.3
17					195.4
18					100.8
19					177.4
20	4.40	1H	brd (8.7)	21,22,23,25	61.1
21					195.5
22	3.18	1H	m	20,21,23,24,25	43.6
	2.16	1H	m	20,23,24,25	
23					75.5
24	1.78	1H	s	22,23,25	28.7
25					179.6

^{1}H and ^{13}C NMR spectra were recorded at 800 MHz and 125 MHz, respectively.

Fig. S19. ^{1}H NMR spectrum of **7** in pyridine-d_5 (800 MHz).

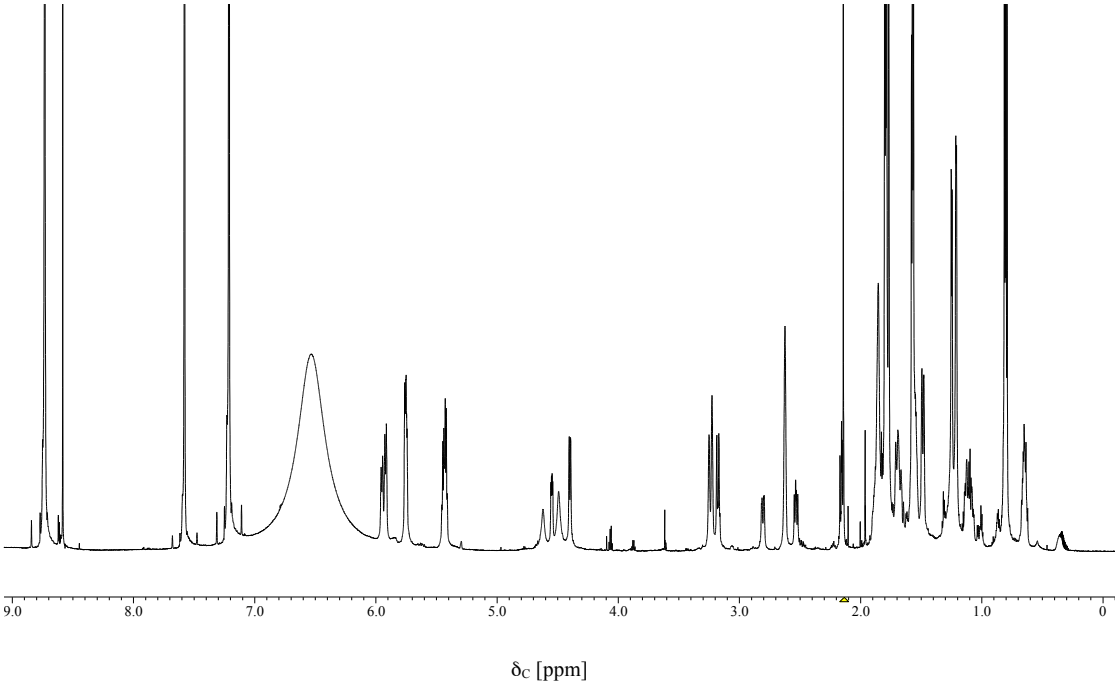

Fig. S20. ^{13}C NMR spectrum of **7** in pyridine-d_5 (125 MHz).

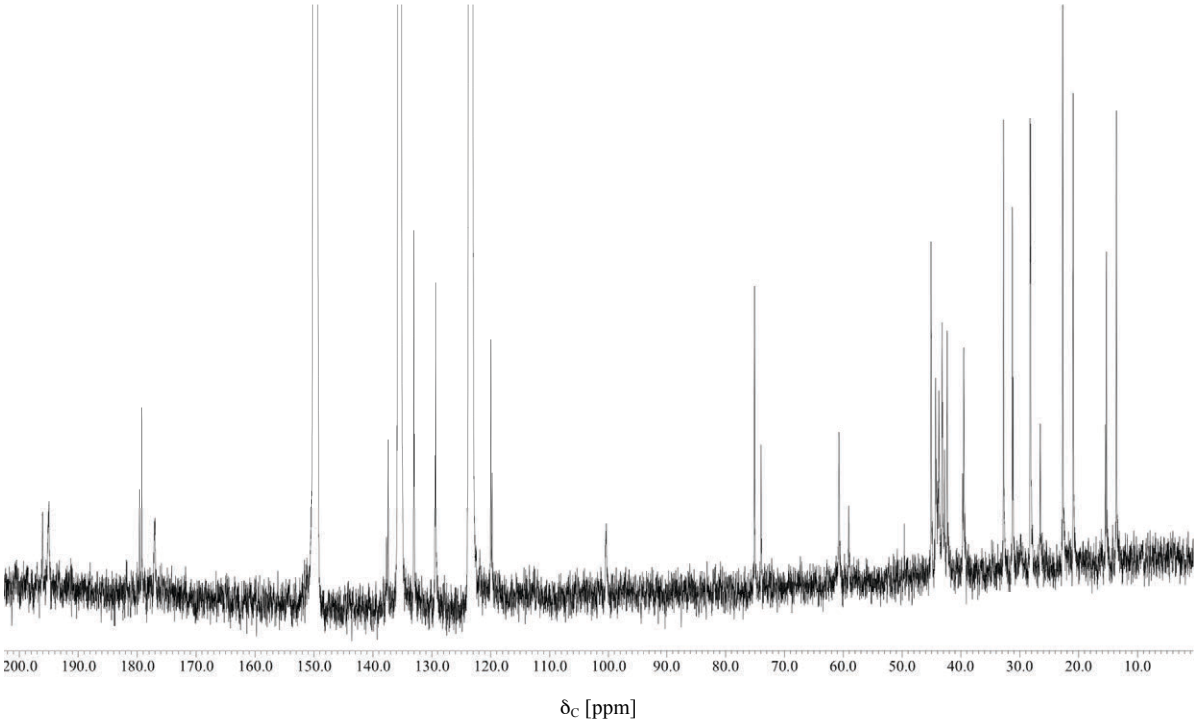

Fig. S21. ^{1}H-^{1}H COSY spectrum of **7** in pyridine-d_5 (500 MHz). COSY, correlated spectroscopy.

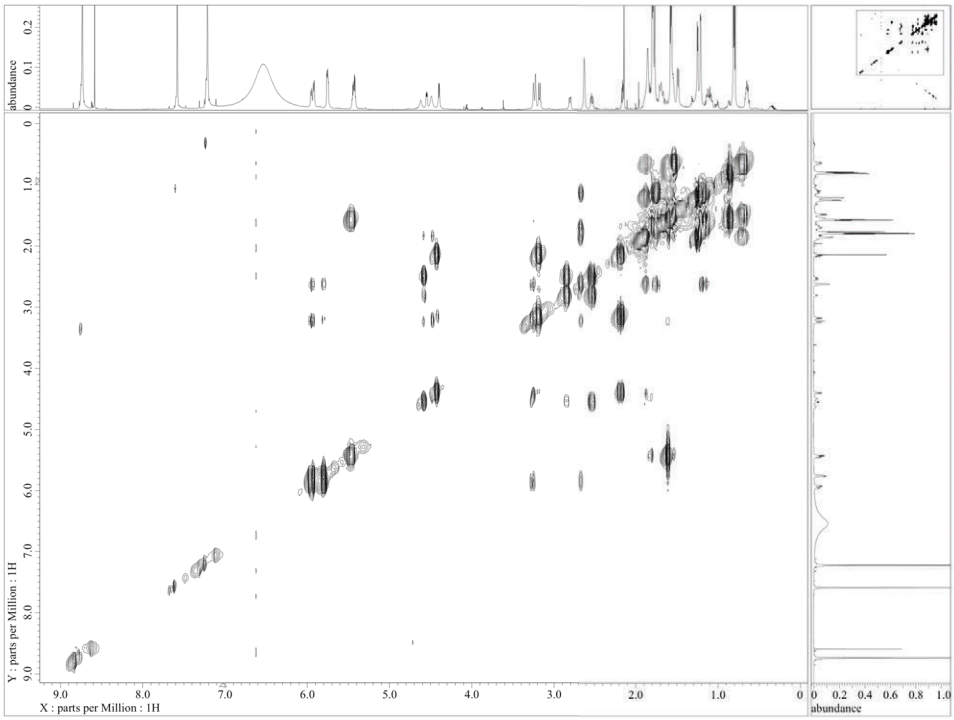

Fig. S22. HMQC spectrum of **7** in pyridine-d_5 (800 MHz). HMQC, heteronuclear multiple quantum coherence.

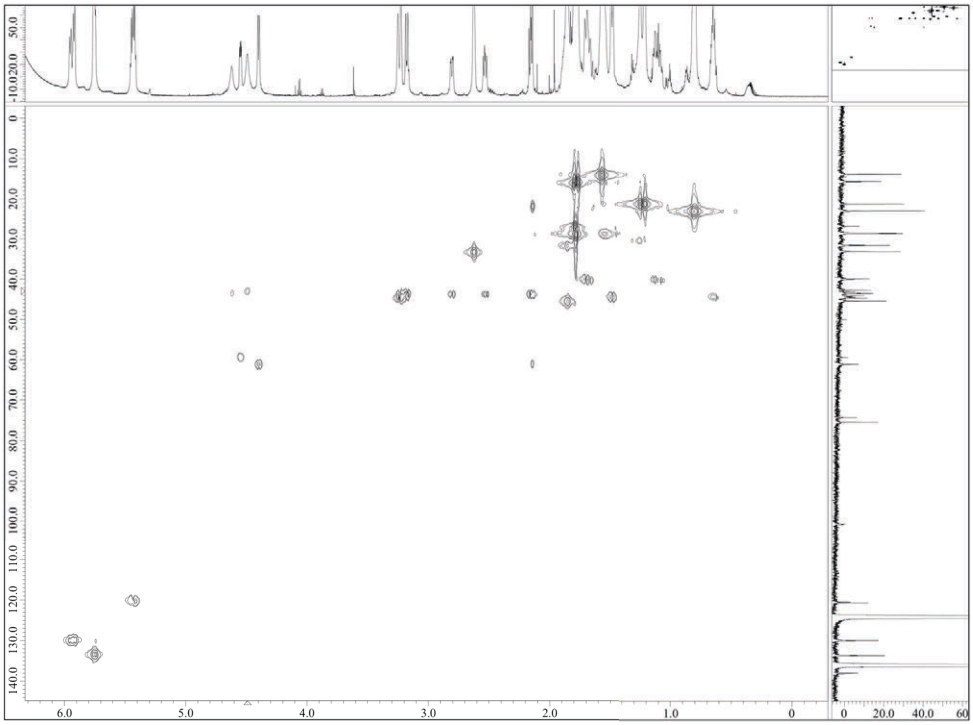

Fig. S23. HMBC spectrum of **7** in pyridine-d_5 (500 MHz). HMBC, heteronuclear multiple bond correlation.

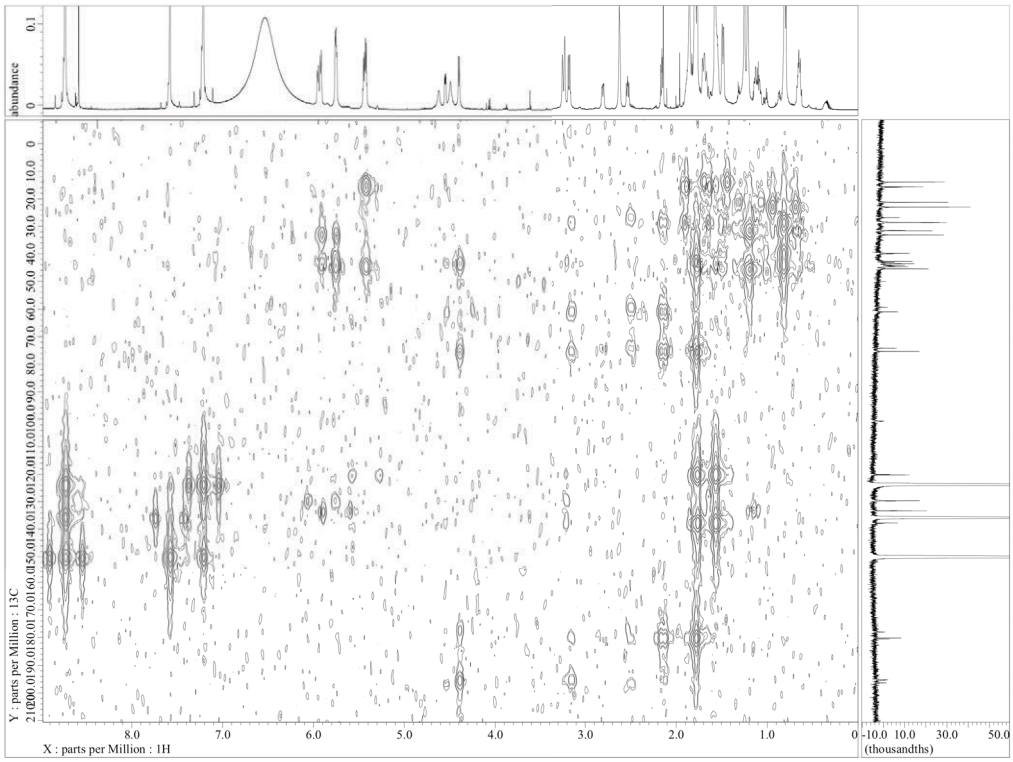

Fig. S24. NOE spectrum of **7** in pyridine-d_5 (600 MHz). NOE, nuclear Overhauser effect.

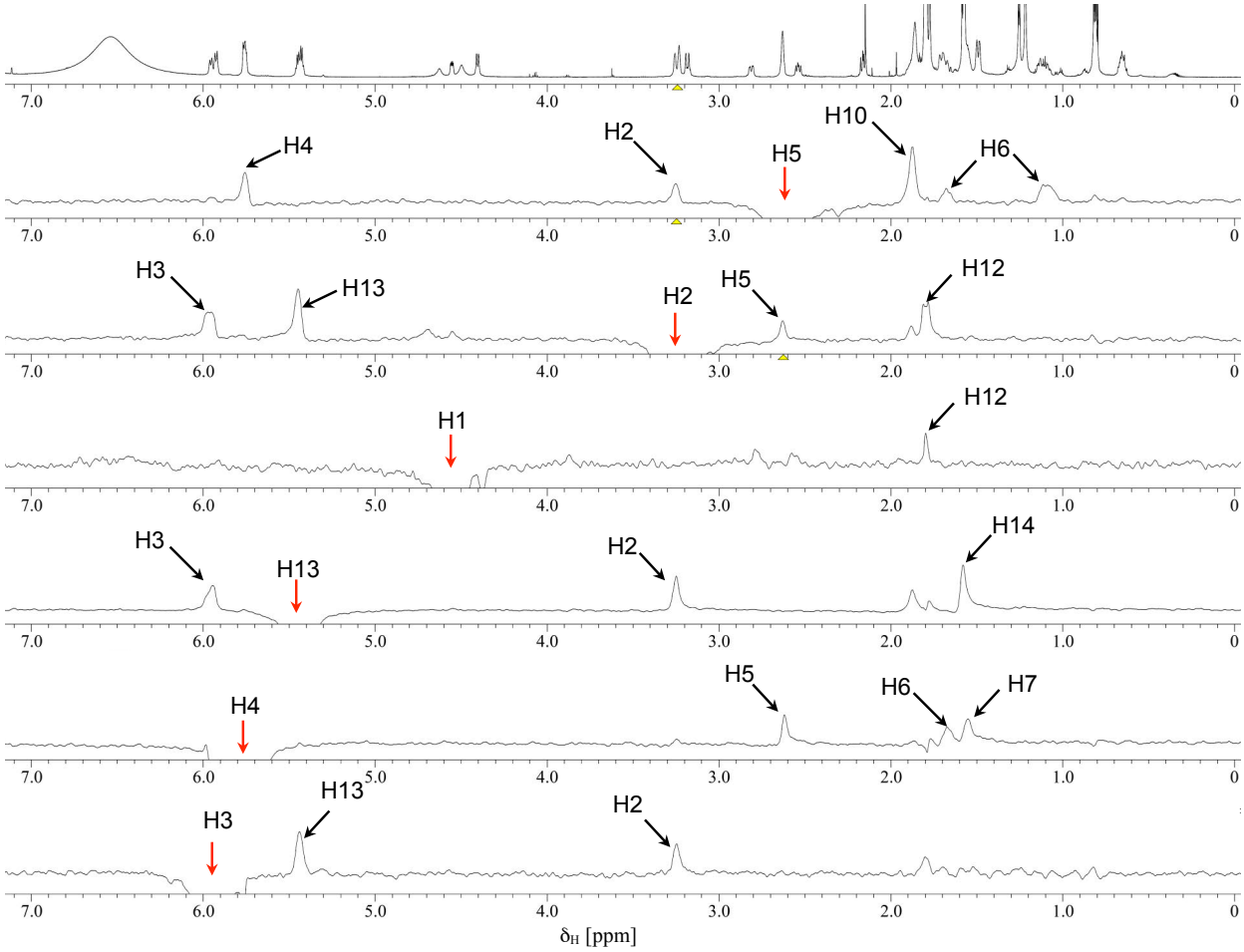

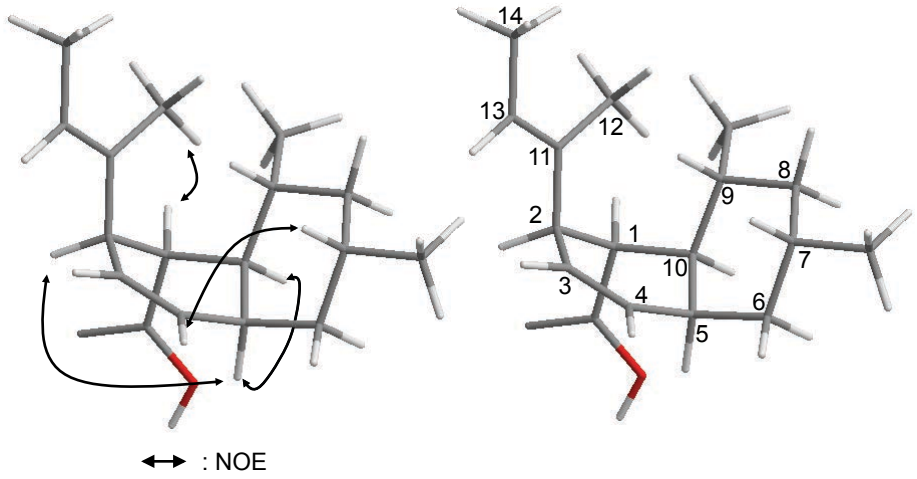

2.6. Crystal structure of **1**.

A colorless prismatic-like specimen of $C_{26}H_{39}NO_7$, approximate dimensions 0.150 mm × 0.180 mm × 0.180 mm, was used for the X-ray crystallographic analysis. The X-ray intensity data were measured.

The total exposure time was 3.33 hours. The frames were integrated with the Bruker SAINT software package using a narrow-frame algorithm. The integration of the data using a monoclinic unit cell yielded a total of 9784 reflections to a maximum θ angle of 68.21° (0.83 Å resolution), of which 4780 were independent (average redundancy 2.047, completeness = 97.1%, R_{int} = 1.42%) and 4614 (96.53 %) were greater than $2\sigma(F^2)$. The final cell constants of a = 11.6604(4) Å, b = 6.2663(2) Å, c = 18.5264(6) Å, β = 93.2160(18)°, volume = 1351.55(8) Å^3, are based upon the refinement of the XYZ-centroids of 6543 reflections above 20 $\sigma(I)$ with 7.593° < 2θ < 136.9°. Data were corrected for absorption effects using the empirical method (SADABS). The ratio of minimum to maximum apparent transmission was 0.909. The calculated minimum and maximum transmission coefficients (based on crystal size) are 0.8860 and 0.9040.

The final anisotropic full-matrix least-squares refinement on F^2 with 317 variables converged at R_1 = 7.01 %, for the observed data and wR_2 = 21.59 % for all data. The goodness-of-fit was 1.133. The largest peak in the final difference electron density synthesis was 0.470 e$^-$/Å^3 and the largest hole was –0.337 e$^-$/Å^3 with an RMS deviation of 0.057 e$^-$/Å^3. On the basis of the final model, the calculated density was 1.174 g/cm^3 and F(000), 516 e$^-$.

Table S5. Sample and crystal data for u131209yag2.

Identification code	u131209yag2	
Chemical formula	$C_{26}H_{39}NO_7$	
Formula weight	477.58	
Temperature	173(2) K	
Wavelength	1.54178 Å	
Crystal size	0.150 × 0.180 × 0.180 mm	
Crystal habit	colorless prismatic	
Crystal system	monoclinic	
Space group	$P2_1$	
Unit cell dimensions	a = 11.6604(4) Å	α = 90°
	b = 6.2663(2) Å	β = 93.2160(18)°
	c = 18.5264(6) Å	γ = 90°
Volume	1351.55(8) Å^3	
Z	2	
Density (calculated)	1.174 g/cm^3	
Absorption	0.690 mm^{-1}	
F(000)	516	

Table S6. Data collection and structure refinement for u131209yag2.

Theta range for data collection	2.39 to 68.21°
Index ranges	–13<=h<=14, –7<=k<=7, –22<=l<=22
Reflections collected	9784
Independent reflections	4780 [R_{int} = 0.0142]
Coverage of independent reflections	97.1%
Absorption correction	empirical
Max. and min. transmission	0.9040 and 0.8860
Refinement method	Full-matrix least-squares on F^2
Refinement program	SHELXL-2013[16]
Function minimized	$\Sigma\, w(F_o^2 - F_c^2)^2$
Data / restraints / parameters	4780 / 190 / 317
Goodness-of-fit on F^2	1.133
Δ/σ_{max}	0.004
Final *R* indices	4614 data; $I > 2\sigma(I)$ R_1 = 0.0701, wR_2 = 0.2115
	all data R_1 = 0.0718, wR_2 = 0.2159
Weighting scheme	$w = 1/[\sigma^2(F_o^2)+(0.1339P)^2+0.4611P]$ where $P=(F_o^2+2F_c^2)/3$
Absolute structure parameter	0.1(1)
Largest diff. peak and hole	0.470 and –0.337 eÅ^{-3}
R.M.S. deviation from mean	0.057 eÅ^{-3}

Table S7. Atomic coordinates and equivalent isotropic atomic displacement parameters (Å^2) for u131209yag2.

U(eq) is defined as one third of the trace of the orthogonalized U_{ij} tensor.

	x/a	y/b	z/c	U(eq)
C1	0.2890(3)	0.2556(6)	0.8730(2)	0.0383(8)
C2	0.4125(3)	0.3616(7)	0.8831(2)	0.0437(9)
C3	0.4086(3)	0.5427(7)	0.9356(3)	0.0487(10)
C4	0.3647(3)	0.5028(7)	0.9986(2)	0.0490(10)
C5	0.3162(3)	0.2853(6)	0.0105(2)	0.0417(9)
N1	0.1121(4)	0.3501(12)	0.6352(2)	0.0807(16)
C6	0.2612(4)	0.2584(8)	0.0825(2)	0.0497(10)
C7	0.2157(4)	0.0332(8)	0.0909(2)	0.0522(10)
C8	0.1296(4)	0.9830(8)	0.0285(2)	0.0505(10)
C9	0.1747(3)	0.0144(6)	0.9531(2)	0.0413(8)
C10	0.2300(3)	0.2341(6)	0.94627(19)	0.0361(8)
C11	0.4676(3)	0.4012(7)	0.8128(3)	0.0491(9)
C12	0.5317(5)	0.2163(9)	0.7843(3)	0.0633(12)
C13	0.4584(5)	0.5886(8)	0.7785(3)	0.0617(12)
C14	0.5060(6)	0.6443(11)	0.7083(4)	0.0808(17)
C15	0.1644(6)	0.9991(11)	0.1632(3)	0.0727(15)
C16	0.0772(4)	0.9813(7)	0.8955(2)	0.0478(9)
C17	0.2167(3)	0.3787(7)	0.8188(2)	0.0418(8)
C18	0.1898(4)	0.3149(9)	0.7491(2)	0.0525(11)
C19	0.1188(4)	0.4445(11)	0.6996(3)	0.0652(14)
C20	0.1779(5)	0.1545(15)	0.6327(3)	0.0857(15)
C21	0.2248(4)	0.1255(13)	0.7112(3)	0.0727(14)
C22	0.2798(5)	0.171(2)	0.5840(3)	0.1076(17)
C23	0.2466(6)	0.161(2)	0.5025(3)	0.1227(17)
C24	0.3540(7)	0.180(3)	0.4596(4)	0.145(3)
C25	0.1869(6)	0.944(2)	0.4865(4)	0.1267(19)
C26	0.1336(9)	0.501(2)	0.3017(5)	0.118(3)
O1	0.1781(3)	0.5631(5)	0.84151(17)	0.0539(8)
O2	0.0693(3)	0.6121(7)	0.7171(2)	0.0724(11)
O3	0.2819(4)	0.9717(8)	0.7314(2)	0.0843(14)
O4	0.1689(4)	0.3430(17)	0.4866(2)	0.135(2)
O5	0.0956(4)	0.9339(18)	0.4544(3)	0.151(3)
O6	0.2473(5)	0.7483(19)	0.5117(3)	0.154(2)
O7	0.1015(7)	0.3527(17)	0.3474(3)	0.169(4)

Table S8. Bond lengths (Å) for u131209yag2.

C1-C17	1.490(5)	C1-C10	1.561(5)
C1-C2	1.588(5)	C1-H1	1.0
C2-C3	1.497(6)	C2-C11	1.505(6)
C2-H2	1.0	C3-C4	1.324(7)
C3-H3	0.95	C4-C5	1.497(6)
C4-H4	0.95	C5-C6	1.522(6)
C5-C10	1.548(5)	C5-H5	1.0
N1-C19	1.330(8)	N1-C20	1.448(10)
N1-H1A	0.88	C6-C7	1.519(7)
C6-H6A	0.99	C6-H6B	0.99
C7-C15	1.513(7)	C7-C8	1.522(6)
C7-H7	1.0	C8-C9	1.532(6)
C8-H8A	0.99	C8-H8B	0.99
C9-C16	1.529(6)	C9-C10	1.529(5)
C9-H9	1.0	C10-H10	1.0
C11-C13	1.336(7)	C11-C12	1.491(7)
C12-H12A	0.98	C12-H12B	0.98
C12-H12C	0.98	C13-C14	1.486(8)
C13-H13	0.95	C14-H14A	0.98
C14-H14B	0.98	C14-H14C	0.98
C15-H15A	0.98	C15-H15B	0.98
C15-H15C	0.98	C16-H16A	0.98
C16-H16B	0.98	C16-H16C	0.98
C17-O1	1.318(5)	C17-C18	1.370(6)
C18-C19	1.449(7)	C18-C21	1.449(8)
C19-O2	1.250(8)	C20-C22	1.534(9)
C20-C21	1.536(7)	C20-H20	1.0
C21-O3	1.219(8)	C22-C23	1.540(8)
C22-H22A	0.99	C22-H22B	0.99
C23-O4	1.474(15)	C23-C24	1.525(11)
C23-C25	1.552(17)	C24-H24A	0.98
C24-H24B	0.98	C24-H24C	0.98
C25-O5	1.191(8)	C25-O6	1.476(16)
C26-O7	1.327(12)	C26-H26A	0.98
C26-H26B	0.98	C26-H26C	0.98
O1-H1B	0.84	O4-H4A	0.84
O6-H6	0.84	O7-H7A	0.84

Table S9. Bond angles (°) for u131209yag2.

C17-C1-C10	111.8(3)	C17-C1-C2	109.7(3)
C10-C1-C2	112.0(3)	C17-C1-H1	107.7

C10-C1-H1	107.7	C2-C1-H1	107.7
C3-C2-C11	117.9(4)	C3-C2-C1	109.4(3)
C11-C2-C1	113.3(3)	C3-C2-H2	105.0
C11-C2-H2	105.0	C1-C2-H2	105.0
C4-C3-C2	117.2(4)	C4-C3-H3	121.4
C2-C3-H3	121.4	C3-C4-C5	118.0(4)
C3-C4-H4	121.0	C5-C4-H4	121.0
C4-C5-C6	114.3(3)	C4-C5-C10	108.0(3)
C6-C5-C10	111.3(3)	C4-C5-H5	107.6
C6-C5-H5	107.6	C10-C5-H5	107.6
C19-N1-C20	113.6(4)	C19-N1-H1A	123.2
C20-N1-H1A	123.2	C7-C6-C5	111.1(3)
C7-C6-H6A	109.4	C5-C6-H6A	109.4
C7-C6-H6B	109.4	C5-C6-H6B	109.4
H6A-C6-H6B	108.0	C6-C7-C15	112.3(4)
C6-C7-C8	109.5(4)	C15-C7-C8	111.5(4)
C6-C7-H7	107.8	C15-C7-H7	107.8
C8-C7-H7	107.8	C7-C8-C9	114.9(4)
C7-C8-H8A	108.5	C9-C8-H8A	108.5
C7-C8-H8B	108.5	C9-C8-H8B	108.5
H8A-C8-H8B	107.5	C16-C9-C10	111.4(3)
C16-C9-C8	109.7(3)	C10-C9-C8	111.0(3)
C16-C9-H9	108.2	C10-C9-H9	108.2
C8-C9-H9	108.2	C9-C10-C5	112.5(3)
C9-C10-C1	111.0(3)	C5-C10-C1	110.6(3)
C9-C10-H10	107.5	C5-C10-H10	107.5
C1-C10-H10	107.5	C13-C11-C12	122.9(4)
C13-C11-C2	122.0(4)	C12-C11-C2	115.1(4)
C11-C12-H12A	109.5	C11-C12-H12B	109.5
H12A-C12-H12B	109.5	C11-C12-H12C	109.5
H12A-C12-H12C	109.5	H12B-C12-H12C	109.5
C11-C13-C14	126.8(5)	C11-C13-H13	116.6
C14-C13-H13	116.6	C13-C14-H14A	109.5
C13-C14-H14B	109.5	H14A-C14-H14B	109.5
C13-C14-H14C	109.5	H14A-C14-H14C	109.5
H14B-C14-H14C	109.5	C7-C15-H15A	109.5
C7-C15-H15B	109.5	H15A-C15-H15B	109.5
C7-C15-H15C	109.5	H15A-C15-H15C	109.5
H15B-C15-H15C	109.5	C9-C16-H16A	109.5
C9-C16-H16B	109.5	H16A-C16-H16B	109.5
C9-C16-H16C	109.5	H16A-C16-H16C	109.5
H16B-C16-H16C	109.5	O1-C17-C18	119.5(4)

O1-C17-C1	115.4(3)	C18-C17-C1	125.1(4)
C17-C18-C19	121.6(5)	C17-C18-C21	129.8(4)
C19-C18-C21	108.6(4)	O2-C19-N1	127.0(5)
O2-C19-C18	124.3(5)	N1-C19-C18	108.7(5)
N1-C20-C22	113.1(8)	N1-C20-C21	103.3(5)
C22-C20-C21	108.5(4)	N1-C20-H20	110.5
C22-C20-H20	110.5	C21-C20-H20	110.5
O3-C21-C18	131.5(4)	O3-C21-C20	122.9(5)
C18-C21-C20	105.5(5)	C20-C22-C23	114.4(5)
C20-C22-H22A	108.7	C23-C22-H22A	108.7
C20-C22-H22B	108.7	C23-C22-H22B	108.7
H22A-C22-H22B	107.6	O4-C23-C24	110.4(10)
O4-C23-C22	106.5(7)	C24-C23-C22	109.9(6)
O4-C23-C25	112.1(6)	C24-C23-C25	110.0(9)
C22-C23-C25	107.8(9)	C23-C24-H24A	109.5
C23-C24-H24B	109.5	H24A-C24-H24B	109.5
C23-C24-H24C	109.5	H24A-C24-H24C	109.5
H24B-C24-H24C	109.5	O5-C25-O6	120.8(12)
O5-C25-C23	121.3(12)	O6-C25-C23	117.9(6)
O7-C26-H26A	109.5	O7-C26-H26B	109.5
H26A-C26-H26B	109.5	O7-C26-H26C	109.5
H26A-C26-H26C	109.5	H26B-C26-H26C	109.5
C17-O1-H1B	109.5	C23-O4-H4A	109.5
C25-O6-H6	109.5	C26-O7-H7A	109.5

Table S10. Torsion angles (°) for u131209yag2.

C17-C1-C2-C3	83.4(4)	C10-C1-C2-C3	-41.4(4)
C17-C1-C2-C11	-50.4(4)	C10-C1-C2-C11	-175.2(3)
C11-C2-C3-C4	-177.0(3)	C1-C2-C3-C4	51.6(5)
C2-C3-C4-C5	-3.7(5)	C3-C4-C5-C6	-176.5(4)
C3-C4-C5-C10	-51.9(4)	C4-C5-C6-C7	-179.2(3)
C10-C5-C6-C7	58.0(4)	C5-C6-C7-C15	177.9(4)
C5-C6-C7-C8	-57.6(4)	C6-C7-C8-C9	54.8(5)
C15-C7-C8-C9	179.8(4)	C7-C8-C9-C16	-174.2(4)
C7-C8-C9-C10	-50.6(5)	C16-C9-C10-C5	171.3(3)
C8-C9-C10-C5	48.6(4)	C16-C9-C10-C1	-64.2(4)
C8-C9-C10-C1	173.1(3)	C4-C5-C10-C9	-179.8(3)
C6-C5-C10-C9	-53.5(4)	C4-C5-C10-C1	55.5(4)
C6-C5-C10-C1	-178.2(3)	C17-C1-C10-C9	100.9(4)
C2-C1-C10-C9	-135.5(3)	C17-C1-C10-C5	-133.6(3)
C2-C1-C10-C5	-9.9(4)	C3-C2-C11-C13	-35.6(6)
C1-C2-C11-C13	94.0(5)	C3-C2-C11-C12	144.8(4)
C1-C2-C11-C12	-85.5(4)	C12-C11-C13-C14	1.3(9)
C2-C11-C13-C14	-178.2(5)	C10-C1-C17-O1	50.2(4)
C2-C1-C17-O1	-74.7(4)	C10-C1-C17-C18	-130.3(4)
C2-C1-C17-C18	104.7(5)	O1-C17-C18-C19	-0.6(7)
C1-C17-C18-C19	180.0(4)	O1-C17-C18-C21	177.6(5)
C1-C17-C18-C21	-1.8(8)	C20-N1-C19-O2	-178.7(6)
C20-N1-C19-C18	-1.4(7)	C17-C18-C19-O2	-6.0(8)
C21-C18-C19-O2	175.4(5)	C17-C18-C19-N1	176.6(5)
C21-C18-C19-N1	-2.0(6)	C19-N1-C20-C22	-113.2(6)
C19-N1-C20-C21	4.0(7)	C17-C18-C21-O3	3.5(11)
C19-C18-C21-O3	-178.1(7)	C17-C18-C21-C20	-174.2(5)
C19-C18-C21-C20	4.2(6)	N1-C20-C21-O3	177.3(6)
C22-C20-C21-O3	-62.4(10)	N1-C20-C21-C18	-4.8(7)
C22-C20-C21-C18	115.5(7)	N1-C20-C22-C23	-76.0(11)
C21-C20-C22-C23	170.0(9)	C20-C22-C23-O4	59.9(12)
C20-C22-C23-C24	179.6(11)	C20-C22-C23-C25	-60.5(11)
O4-C23-C25-O5	11.1(9)	C24-C23-C25-O5	-112.2(9)
C22-C23-C25-O5	128.0(8)	O4-C23-C25-O6	-169.5(6)
C24-C23-C25-O6	67.2(9)	C22-C23-C25-O6	-52.6(8)

Table S11. Anisotropic atomic displacement parameters (Å^2) for u131209yag2.

The anisotropic atomic displacement factor exponent takes the form: $-2\pi^2[\ h^2\ a^{*2}\ U_{11} + ... + 2\ h\ k\ a^*\ b^*\ U_{12}\ ]$

	U_{11}	U_{22}	U_{33}	U_{23}	U_{13}	U_{12}
C1	0.0303(17)	0.0428(19)	0.0412(17)	-0.0062(15)	-0.0028(14)	0.0018(14)
C2	0.0302(17)	0.046(2)	0.054(2)	-0.0005(17)	-0.0036(15)	0.0017(15)
C3	0.0365(19)	0.048(2)	0.061(2)	-0.0063(18)	-0.0096(18)	-0.0057(16)
C4	0.038(2)	0.055(2)	0.052(2)	-0.0132(18)	-0.0116(17)	-0.0032(17)
C5	0.0327(17)	0.050(2)	0.0413(18)	-0.0071(16)	-0.0073(15)	0.0093(15)
N1	0.048(2)	0.159(5)	0.0349(17)	0.008(2)	-0.0029(16)	0.017(3)
C6	0.047(2)	0.062(2)	0.0389(19)	-0.0060(18)	-0.0052(16)	0.0085(19)
C7	0.056(2)	0.059(2)	0.041(2)	0.0026(18)	-0.0006(18)	0.013(2)
C8	0.052(2)	0.052(2)	0.048(2)	0.0034(18)	0.0052(18)	-0.0013(18)
C9	0.0416(19)	0.0393(19)	0.0428(19)	-0.0019(15)	0.0009(16)	0.0029(15)
C10	0.0315(17)	0.0378(17)	0.0384(17)	-0.0047(14)	-0.0054(14)	0.0047(13)
C11	0.0339(18)	0.053(2)	0.060(2)	0.0002(19)	0.0050(17)	-0.0011(17)
C12	0.057(3)	0.064(3)	0.071(3)	-0.003(2)	0.019(2)	0.004(2)
C13	0.058(3)	0.060(3)	0.069(3)	0.005(2)	0.021(2)	0.004(2)
C14	0.089(4)	0.075(3)	0.082(4)	0.009(3)	0.039(3)	0.004(3)
C15	0.084(4)	0.087(4)	0.047(3)	0.007(2)	0.005(2)	0.006(3)
C16	0.047(2)	0.047(2)	0.050(2)	-0.0041(17)	0.0000(18)	-0.0049(17)
C17	0.0333(17)	0.049(2)	0.0433(19)	0.0041(16)	0.0019(15)	0.0021(16)
C18	0.034(2)	0.084(3)	0.0399(19)	0.0052(19)	0.0010(16)	0.0048(19)
C19	0.036(2)	0.116(4)	0.044(2)	0.014(2)	0.0012(19)	0.008(2)
C20	0.049(2)	0.165(4)	0.043(2)	-0.024(2)	-0.0033(18)	0.016(3)
C21	0.046(2)	0.131(4)	0.040(2)	-0.023(2)	-0.0028(18)	0.011(3)
C22	0.054(2)	0.218(4)	0.050(2)	-0.028(3)	0.001(2)	0.009(3)
C23	0.057(2)	0.257(4)	0.054(2)	-0.033(3)	0.003(2)	0.001(3)
C24	0.080(4)	0.291(9)	0.064(3)	-0.031(5)	0.017(3)	-0.007(5)
C25	0.060(3)	0.269(5)	0.050(3)	-0.039(3)	-0.005(2)	-0.003(3)
C26	0.123(7)	0.153(8)	0.081(5)	-0.018(5)	0.026(5)	-0.047(6)
O1	0.0553(18)	0.0523(16)	0.0527(16)	0.0039(13)	-0.0084(14)	0.0128(13)
O2	0.0516(19)	0.104(3)	0.0600(19)	0.0276(19)	-0.0071(16)	0.0152(19)
O3	0.078(3)	0.112(3)	0.061(2)	-0.035(2)	-0.0136(19)	0.033(2)
O4	0.070(3)	0.290(6)	0.0447(19)	-0.013(3)	-0.0035(19)	-0.009(4)
O5	0.068(2)	0.311(8)	0.072(3)	-0.002(4)	-0.025(2)	-0.031(4)
O6	0.072(3)	0.295(7)	0.091(3)	-0.051(5)	-0.013(3)	0.005(4)
O7	0.170(6)	0.278(10)	0.055(2)	0.020(4)	-0.032(3)	-0.145(7)

Table S12. Hydrogen atomic coordinates and isotropic atomic displacement parameters (Å^2) for u131209yag2.

	x/a	y/b	z/c	U(eq)
H1	0.2990	0.1086	0.8533	0.046
H2	0.4618	0.2510	0.9084	0.052

	x/a	y/b	z/c	U(eq)
H3	0.4364	0.6804	0.9242	0.058
H4	0.3640	0.6091	1.0351	0.059
H5	0.3808	0.1806	1.0092	0.05
H1A	0.0716	0.4017	0.5977	0.097
H6A	0.3187	0.2896	1.1225	0.06
H6B	0.1973	0.3615	1.0855	0.06
H7	0.2819	-0.0674	1.0879	0.063
H8A	0.0613	0.0749	1.0328	0.061
H8B	0.1044	-0.1671	1.0330	0.061
H9	0.2348	-0.0963	0.9459	0.05
H10	0.1673	0.3428	0.9464	0.043
H12A	0.5412	0.2362	0.7326	0.095
H12B	0.4886	0.0846	0.7918	0.095
H12C	0.6073	0.2066	0.8099	0.095
H13	0.4171	0.6976	0.8015	0.074
H14A	0.5455	0.5199	0.6893	0.121
H14B	0.5607	0.7623	0.7153	0.121
H14C	0.4434	0.6873	0.6738	0.121
H15A	0.2227	0.0280	1.2022	0.109
H15B	0.1380	-0.1489	1.1667	0.109
H15C	0.0992	0.0960	1.1676	0.109
H16A	0.0222	0.0992	0.8976	0.072
H16B	0.0381	-0.1538	0.9046	0.072
H16C	0.1087	-0.0228	0.8476	0.072
H20	0.1271	0.0322	0.6174	0.103
H22A	0.3339	0.0526	0.5964	0.129
H22B	0.3207	0.3064	0.5947	0.129
H24A	0.3424	0.1022	0.4139	0.217
H24B	0.4198	0.1198	0.4878	0.217
H24C	0.3688	0.3310	0.4495	0.217
H26A	0.0676	0.5911	0.2871	0.177
H26B	0.1629	0.4326	0.2589	0.177
H26C	0.1941	0.5895	0.3253	0.177
H1B	0.1427	0.6264	0.8071	0.081
H4A	0.1421	0.3347	0.4437	0.203
H6	0.2163	-0.3585	0.4912	0.23
H7A	0.0310	0.3278	0.3399	0.253

2.7. Computational analysis of the [4+2] cycloaddition reaction.

In addition to modeling the [4+2] cycloaddition reaction of **10** (see the main text for details), we also computed the reaction profile of substrate **11**, which features thepyrrolidine-2,4-dione moiety. (See Figure 5B for structures of **10** and **11**.) Substrate **11** was examined to account for the possibility that the nonenzymatic cycloaddition occurs after the substrate was cleaved from its carrier protein, since the formation of the pyrrolidinedione releases the substrate. The transition structures of the [4+2] cycloaddition of **11** are shown in Figure S1.

At the SMD^{water}/M06-2X/6-31+G(d,p) level, computations show that the cycloaddition of **11** is about 6 to 8 kcal/mol lower than the reaction of **10**, corresponding to a reactivity difference of approximately 20,000 to 500,000-fold for the two substrates. The conjugated pyrrolidine activates the dienophile to a greater extent than the bare ketone of **10** does. As a result, the transition states of **11** are significantly more polarized than those of **10**. **TS11**$_{endo1}$, **TS11**$_{exo1}$, **TS11**$_{endo2}$, and **TS11**$_{exo2}$ are significantly more asynchronous (ca. 0.2 Å) than the corresponding transition state of **10**. Although the reaction of **11** is significantly more facile, we cannot definitively conclude that it this form of the ketide intermediate undergoes cycloaddition as formation of pyrrolidine-2,4-dione group or some other mechanistic step may be rate-determining for *ΔcghA* strain. Based on the computed transition states, the stereoselectivity of the reaction of **11** is in poorer agreement with experiment. Although **TS11**$_{endo1}$ and **TS11**$_{exo1}$ are still significantly more stable than the alternative *endo* and *exo* transition states, they are isoenergetic, suggesting 1:1 mixture of both **1** and its diastereomer **7** should be expected. The increased stability of **TS11**$_{exo1}$ may be due to stabilizing dispersion interactions between the triene and the pyrrolidinedione moiety. However, **1** is the observed major product of the nonenzymatic cycloaddition, suggesting that cycloaddition of **10** is more likely.

QM Computations.

All computations were performed with *Gaussian09* (Revision D.01)[17] using UCLA's Hoffman2 Beowulf cluster and with the Gordon and Stampede supercomputing cluster located the San Diego Supercomputing Center and Texas Advanced Computing Center, respectively. Geometry optimizations and frequency calculations were performed using the meta-hybrid M06-2X[18] density functional and the double-ζ 6-31+G(d,p) basis set with an

ultrafine integration grid consisting of 590 radial shells and 99 grid points per shell. The SMD solvation model[19] was used to account for the effect of solvation in water. Based on normal vibrational mode analysis, all minima and transition states possess no or one imaginary frequencies, respectively. Thermal corrections were calculated using unscaled M06-2X/6-31+G(d,p) frequencies assuming a standard state of 298.15 K and 1 M. Errors in the calculations of vibrational entropy due to the breakdown of harmonic oscillator approximation for low frequency vibrations was reduced by using Truhlar's quasiharmonic approximation.[20,21] Avogadro[22,23] and Gaussview[24] were used to generate starting geometries for this work. CYLview[25] was used to generate the images presented in this report.

Conformational Analysis

Conformers of the model substrate **10** and **11** were sampled using the mix torsional/low-mode sampling approach implemented in Macromodel V 10.2.[26,27] 16,000 Monte Carlo steps were taken in the simulation. Only conformers differing in maximum atomic deviation by at least 0.5 Å were considered unique structures. Force field geometry optimizations were performed using the Polak–Ribiere conjugate gradient (PRCG) minimizer with a gradient-based convergence threshold of 0.0012 kcal/mol/Å (0.005 kJ/mol/Å). The conformer library consisted of all unique structures no more than 25 kcal/mol higher in energy than the global minimum. The simulations yielded 4515 and 7267 unique conformers of **10** and **11**, respectively, within this range. These sizable libraries were refined using a RMSD filter of 1.5 Å; structures differing in RMSD by 1.5 Å after superposition were deemed unique. The second filter reduced the size of the libraries of **10** and **11** to 118 and 193 structures, respectively, which were subsequently re-optimized using the TPSSTPSS-D3/6-31+G(d,p) model chemistry. Conformers of either substrate within 3 kcal/mol of the TPSSTPSS-D3/6-31+G(d,p) electronic energy of global minimum were subsequently re-optimized at SMD^{water}/M06-2X/6-31+G(d,p) level.

Figure S25. Transition structures and activation free energies of the intramolecular [4+2] cycloaddition reaction of **11** that result in cycloadducts **15a**–**d** computed using SMD^{water}/M06-2X/6-31+G(d,p). Forming bond lengths for each transition structure are given. Products derived from each transition structure are shown below the corresponding transition structure. Gibbs free energies are reported in kcal/mol.

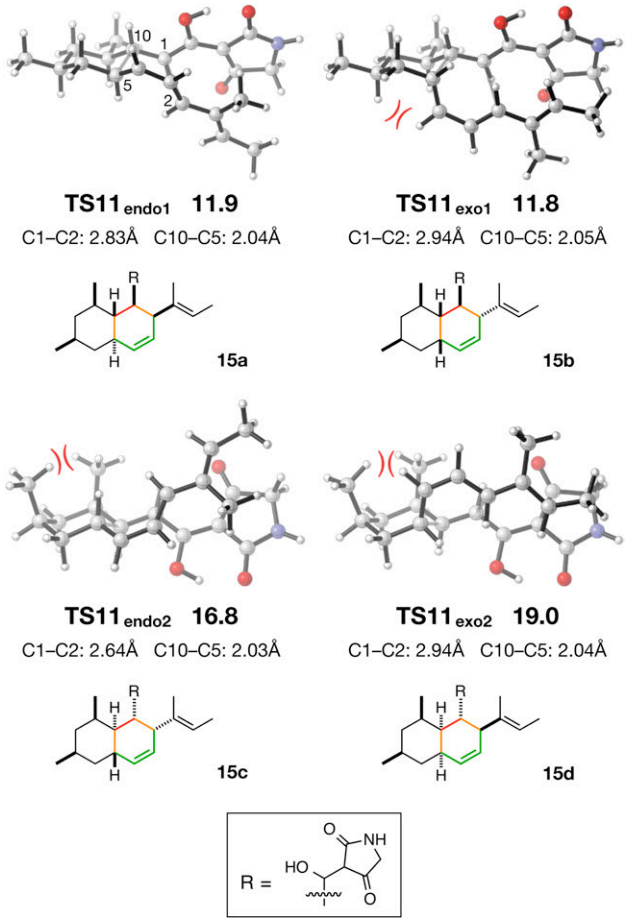

2.8. Cartesian coordinates of the computed structures.

Self-Consistent Field (SCF) energies, as well as zero point energy (ZPE), thermal, and quasiharmonic corrections for each stationary point are also given at the end of the coordinates. Imaginary frequencies of transition structures are also given.

10

C	-1.46571	-1.19966	0.82830
C	-2.73599	-0.68039	1.52311
C	-3.28480	0.49766	0.77848
C	0.77813	-1.10949	-1.22863
C	-1.64336	-1.61134	-0.63723
H	-3.49526	-1.47100	1.54089
H	-0.69427	-0.42050	0.89872
H	-1.09379	-2.06460	1.39681
H	-1.93216	-0.72181	-1.21753
H	0.00757	-3.01451	-0.64342
H	-0.50479	-2.46842	-2.24471
C	-0.31517	-2.13390	-1.21545
C	-4.51812	0.57020	0.25721
C	1.96937	-1.24636	-0.62418
C	4.21298	-0.39374	-0.05203
C	3.02016	-0.23675	-0.66069
C	-2.73428	-2.66890	-0.80233
H	-2.78273	-3.01764	-1.83907
H	-3.72194	-2.28073	-0.53511
H	-2.52803	-3.53626	-0.16271
C	-5.03227	1.74693	-0.46688
O	-6.17513	1.72202	-0.92875
C	5.31230	0.57815	-0.05527
C	6.43698	0.27108	0.62417
H	6.45242	-0.69156	1.13700
C	7.68337	1.08642	0.77459
H	8.55116	0.52485	0.41001
H	7.87447	1.29709	1.83324
H	7.64637	2.03718	0.24096
C	5.10117	1.85679	-0.82275
H	5.97443	2.50829	-0.79514
H	4.24883	2.41300	-0.41684
H	4.87110	1.64126	-1.87205
C	-2.41880	-0.27013	2.96698
H	-1.68951	0.54736	2.98376
H	-3.31934	0.06306	3.49097
H	-1.99396	-1.11704	3.51485
C	-4.16303	2.96361	-0.63879
H	-3.85998	3.35453	0.33683

H	-3.25287	2.70397	-1.18769
H	-4.71382	3.72903	-1.18565
H	4.39541	-1.31902	0.49708
H	2.80119	0.67440	-1.21741
H	0.57148	-0.18566	-1.77453
H	2.18543	-2.16225	-0.07056
H	-5.21211	-0.26436	0.34536
H	-2.60187	1.34411	0.67429

SCF energy: –777.635935 hartree
zero-point correction: +0.418388 hartree
enthalpy correction: +0.442458 hartree
free energy correction: +0.364002 hartree
quasiharmonic free energy correction: +0.369674 hartree

11

C	-4.19581	-0.75621	0.58198
C	-3.74321	0.66368	0.99272
C	-2.26894	0.70433	1.24165
C	-1.74968	-1.68427	-1.10598
C	-4.22859	-1.03605	-0.92586
H	-3.99226	1.37230	0.19216
H	-3.55980	-1.50098	1.08320
H	-5.21111	-0.91361	0.96705
H	-4.91948	-0.30911	-1.37501
H	-3.03869	-1.09168	-2.69943
H	-2.57814	0.20988	-1.61179
C	-2.87757	-0.84535	-1.63966
C	-1.39511	1.51804	0.62741
C	-0.47769	-1.25829	-1.03849
C	1.89814	-1.57344	-0.46960
C	0.63351	-2.04120	-0.51631
C	-4.79514	-2.43456	-1.18047
H	-4.84993	-2.64615	-2.25354
H	-5.80358	-2.52836	-0.76459
H	-4.17379	-3.20824	-0.71559
C	0.02798	1.43768	0.89409
O	0.40447	0.72317	1.94644
C	3.06236	-2.29572	0.05416
C	4.26434	-1.68404	0.01349
H	4.28929	-0.67891	-0.41006
C	5.58627	-2.20789	0.48025
H	5.53056	-3.21756	0.88960
H	6.00586	-1.54971	1.25005
H	6.30586	-2.21480	-0.34649
C	2.82828	-3.67803	0.60397
H	3.74418	-4.13887	0.97357
H	2.40463	-4.33301	-0.16557

H	2.10626	-3.64686	1.42753
C	-4.45762	1.09594	2.28337
H	-4.24697	0.38778	3.09260
H	-4.13507	2.09026	2.60569
H	-5.53944	1.11685	2.12177
C	0.98833	2.03608	0.09876
H	2.09186	-0.57117	-0.85877
H	0.40021	-3.03904	-0.14516
H	-1.98002	-2.69664	-0.76903
H	-0.23983	-0.24720	-1.37912
H	-1.70684	2.20472	-0.15265
H	-1.90133	0.00067	1.99077
C	2.41812	1.90076	0.37842
C	0.84683	2.76950	-1.13914
H	1.39793	0.72867	1.99437
N	3.10763	2.53967	-0.58311
C	2.25489	3.11746	-1.61014
O	2.91127	1.28900	1.35330
O	-0.16556	3.07946	-1.76493
H	4.11935	2.54205	-0.61399
H	2.36992	4.20269	-1.67858
H	2.43739	2.67465	-2.59330

SCF energy: –1097.696094 hartree
zero-point correction: +0.463457 hartree
enthalpy correction: +0.491717 hartree
free energy correction: +0.405061 hartree
quasiharmonic free energy correction: +0.411052 hartree

TS10$_{endo1}$

C	-3.48323	0.74437	-0.59867
C	-2.05147	1.25287	-0.79482
C	-1.10536	0.76350	0.29937
C	-1.28359	-1.23008	0.07825
C	-3.65737	-0.77040	-0.68803
H	-1.67247	0.89924	-1.76468
H	-3.83880	1.08481	0.38698
H	-4.12805	1.22217	-1.34704
H	-1.00440	-1.15596	-0.97298
H	-3.35342	-1.08824	-1.69694
H	-1.54405	0.76246	1.29870
H	-3.02615	-1.19445	1.33702
H	-2.93641	-2.57161	0.24068
C	-2.75606	-1.49089	0.31324
C	0.24412	1.14596	0.24532
C	-0.33743	-1.79898	0.93490
H	-0.68424	-2.22117	1.87760

C	1.59035	-1.02670	-0.34429
C	1.04875	-1.70928	0.72605
H	1.70446	-2.07348	1.51281
H	0.95906	-0.78657	-1.19507
H	0.67169	1.54090	-0.67278
C	-5.11861	-1.15942	-0.47755
H	-5.25885	-2.24101	-0.57511
H	-5.76797	-0.66541	-1.20762
H	-5.45355	-0.86515	0.52450
C	1.03769	1.20492	1.44200
O	0.61600	0.77136	2.53998
C	2.38872	1.87718	1.37742
C	3.02014	-0.79555	-0.54703
C	3.40773	-0.24735	-1.71935
H	2.61837	-0.00388	-2.43204
C	4.79449	0.08207	-2.17049
H	4.98954	-0.37181	-3.14847
H	5.56679	-0.25546	-1.47828
H	4.90283	1.16510	-2.30614
C	3.95707	-1.17203	0.57054
H	4.97671	-0.83282	0.38736
H	3.97904	-2.25872	0.71134
H	3.61982	-0.73498	1.51667
C	-2.06041	2.78777	-0.81171
H	-2.38094	3.17814	0.16140
H	-1.06909	3.19342	-1.02959
H	-2.75894	3.15556	-1.57062
H	2.24187	2.95250	1.53344
H	2.86879	1.74291	0.40485
H	3.03723	1.50496	2.17323

SCF energy: –777.610286 hartree
zero-point correction: +0.418637 hartree
enthalpy correction: +0.440819 hartree
free energy correction: +0.369548 hartree
quasiharmonic free energy correction: +0.372530 hartree
imaginary frequency: –448.2096

TS10$_{exo1}$

C	-0.62079	-1.79691	0.59339
C	-1.60698	-1.13180	-0.10696
C	-0.24732	1.16356	0.25935
C	1.08637	0.86903	-0.06451
C	1.22862	-0.97776	-0.82239
C	0.73076	-1.78257	0.20481
H	-0.87121	-2.27859	1.53569
H	1.43780	-2.30082	0.84956
C	2.14087	0.90185	1.03413

H	1.84172	0.19209	1.81847
C	2.68258	-1.07475	-1.23838
H	2.85600	-2.05251	-1.70702
H	2.88402	-0.31874	-2.00892
C	3.67344	-0.87165	-0.08783
C	3.53313	0.52805	0.51202
H	3.81816	1.26618	-0.25507
H	4.25295	0.63669	1.33315
H	-1.40694	-0.82189	-1.12994
H	-0.57065	1.13914	1.29648
C	-1.17298	1.68150	-0.70703
O	-0.94424	1.67872	-1.93994
H	1.42354	1.28414	-1.01846
H	0.54251	-0.72448	-1.62980
H	3.45928	-1.60810	0.69894
C	5.10292	-1.10051	-0.57422
H	5.22941	-2.11247	-0.97284
H	5.82332	-0.96316	0.23875
H	5.35429	-0.39010	-1.37110
C	-2.99858	-1.01893	0.31998
C	-3.90171	-0.60749	-0.59761
H	-3.52195	-0.39435	-1.59813
C	-5.36922	-0.39083	-0.41697
H	-5.93615	-1.03223	-1.10148
H	-5.62807	0.64279	-0.67590
H	-5.71384	-0.58644	0.59920
C	-3.32086	-1.34460	1.75432
H	-4.36550	-1.15010	1.99702
H	-2.69514	-0.74779	2.42812
H	-3.11496	-2.39809	1.97297
C	-2.45447	2.29606	-0.20098
H	-3.27773	2.07256	-0.88502
H	-2.32039	3.38420	-0.17670
H	-2.70763	1.95658	0.80566
C	2.19812	2.30597	1.65014
H	1.24343	2.58577	2.10382
H	2.44046	3.05025	0.88239
H	2.97376	2.35043	2.42199

SCF energy: –777.608113 hartree
zero-point correction: +0.418789 hartree
enthalpy correction: +0.440896 hartree
free energy correction: +0.370082 hartree
quasiharmonic free energy correction: +0.372511 hartree
imaginary frequency: –445.0164

TS10$_{endo2}$

C	-3.60778	0.03531	0.97848

C	-2.18103	-0.13711	1.52800
C	-1.16642	0.73514	0.78734
C	-1.41100	0.15569	-1.10441
C	-3.85067	-0.29043	-0.50007
H	-2.22157	0.30041	2.53628
H	-3.88418	1.08719	1.13343
H	-4.28867	-0.56137	1.59845
H	-1.20428	-0.88362	-0.85669
H	-4.85239	0.09192	-0.73587
H	-1.53348	1.74201	0.58416
H	-3.07660	0.22429	-2.44428
H	-3.02368	1.55124	-1.28674
C	-2.86605	0.46982	-1.39499
C	-3.87338	-1.78926	-0.81614
H	-4.22783	-1.95359	-1.83960
H	-4.55124	-2.31782	-0.13716
H	-2.88888	-2.25747	-0.73088
C	0.18862	0.68107	1.16067
C	-0.41620	0.80290	-1.84620
H	-0.69796	1.66910	-2.44426
C	1.42406	-0.46377	-0.86956
C	0.94968	0.49317	-1.74385
H	1.65497	1.13019	-2.27176
C	1.04697	1.80490	0.92009
H	0.58343	-0.14624	1.74287
O	0.66761	2.79830	0.25469
H	0.73082	-1.18460	-0.44470
C	2.83872	-0.74522	-0.62827
C	3.14195	-1.81313	0.14199
H	2.30188	-2.38734	0.53650
C	3.85338	0.17658	-1.25154
H	3.82394	0.10252	-2.34468
H	4.86965	-0.04506	-0.92525
H	3.63373	1.21893	-0.99589
C	4.49453	-2.32022	0.52679
H	4.62343	-3.35142	0.17760
H	4.59298	-2.34853	1.61827
H	5.31206	-1.72088	0.12398
C	2.42388	1.80867	1.54092
H	2.83892	0.80107	1.62512
H	2.34341	2.22368	2.55260
H	3.09697	2.44733	0.96503
C	-1.72993	-1.58990	1.71841
H	-0.90399	-1.65189	2.43331
H	-2.55470	-2.19014	2.11632
H	-1.39363	-2.06162	0.79035

SCF energy: –777.604266 hartree
zero-point correction: +0.419344 hartree
enthalpy correction: +0.441377 hartree

free energy correction: +0.370610 hartree
quasiharmonic free energy correction: +0.373232 hartree
imaginary frequency: –462.5039

TS10$_{exo2}$

C	-3.85350	-0.20996	-0.67498
C	-2.71451	-0.26625	-1.70827
C	-1.30011	-0.39795	-1.16954
C	-1.11338	1.11170	0.10479
C	-3.63799	0.93793	0.31916
H	-0.55043	0.06692	-1.80994
H	-2.75607	0.65892	-2.29535
H	-2.90572	-1.08836	-2.41007
H	-4.74810	0.05627	-1.25354
H	-1.30146	1.81822	-0.70736
H	-3.73790	1.87994	-0.23684
C	0.19986	1.17445	0.60860
H	0.42831	0.79440	1.59956
C	-0.87728	-1.54863	-0.49247
H	-1.62143	-2.25784	-0.14152
C	0.45241	-1.76587	-0.09123
H	0.64177	-2.57294	0.61290
C	1.49516	-0.94535	-0.47119
H	1.35888	-0.28146	-1.32151
C	1.23570	1.89753	-0.06676
C	-4.18451	-1.54621	-0.00076
H	-4.30668	-2.33783	-0.74855
H	-5.12834	-1.45679	0.54823
H	-3.42807	-1.87296	0.71408
O	1.12396	2.32283	-1.24334
C	-2.29288	1.00302	1.06577
H	-2.31055	1.97958	1.57247
H	-4.44531	0.92721	1.06229
C	2.86750	-1.07702	0.00822
C	3.83697	-0.44749	-0.69237
H	3.51924	0.12411	-1.56576
C	3.10038	-1.88971	1.25457
H	4.12921	-1.81881	1.60770
H	2.87421	-2.94802	1.08348
H	2.43957	-1.54529	2.05832
C	5.30680	-0.43166	-0.42334
H	5.85338	-0.80016	-1.29874
H	5.59668	-1.03383	0.43851
H	5.64843	0.59715	-0.25702
C	2.49954	2.20038	0.70112
H	2.41721	3.21715	1.10368
H	3.36419	2.17086	0.03248
H	2.65254	1.51075	1.53419

C	-2.10368	-0.04164	2.16906
H	-1.32847	0.27209	2.87482
H	-3.03340	-0.16699	2.73354
H	-1.81234	-1.01860	1.77448

SCF energy: –777.598201 hartree
zero-point correction: +0.420094 hartree
enthalpy correction: +0.441963 hartree
free energy correction: +0.371625 hartree
quasiharmonic free energy correction: +0.374227 hartree
imaginary frequency: –457.3105

10' (reactive conformer)

C	-1.42752	-1.97194	0.24130
C	-2.04276	-1.04793	-0.52331
C	0.75313	1.46612	1.07913
C	1.50493	1.62690	-0.01836
C	0.93408	-1.81440	-0.61463
C	-0.01477	-2.36626	0.15932
H	-2.00002	-2.47282	1.01956
H	0.28285	-3.17237	0.83028
C	2.99478	1.49574	-0.10879
H	3.41761	1.46856	0.90389
C	2.38340	-2.19202	-0.54016
H	2.48766	-3.10376	0.06027
H	2.78406	-2.40611	-1.54112
C	3.22584	-1.06723	0.09388
C	3.34470	0.17153	-0.82015
H	2.70277	0.07436	-1.70604
H	4.37318	0.24597	-1.19632
H	-1.48048	-0.54379	-1.31089
H	1.19775	1.20107	2.03646
C	-0.72285	1.59995	1.02742
O	-1.29628	2.11261	0.06675
H	0.99812	1.85061	-0.96093
H	0.67388	-0.99269	-1.28440
H	2.70618	-0.76715	1.01514
C	4.61165	-1.58133	0.48395
H	4.54522	-2.39681	1.21133
H	5.21299	-0.77908	0.92576
H	5.14478	-1.95354	-0.39894
C	-3.43986	-0.62413	-0.37602
C	-3.90121	0.33757	-1.20303
H	-3.19646	0.73082	-1.93717
C	-5.26242	0.95885	-1.23980
H	-5.19192	2.03548	-1.04408
H	-5.95624	0.52797	-0.51656

H	-5.70199	0.85442	-2.23827
C	-4.25479	-1.27568	0.71008
H	-5.27289	-0.88896	0.75406
H	-3.78877	-1.11542	1.68940
H	-4.30905	-2.35920	0.55623
C	-1.48966	1.10620	2.22086
H	-1.15763	0.10043	2.49719
H	-2.56189	1.11271	2.01713
H	-1.27336	1.76396	3.07122
C	3.56820	2.69494	-0.86977
H	3.29026	3.64057	-0.39466
H	3.19434	2.70785	-1.89991
H	4.66008	2.63476	-0.90416

SCF energy: –777.630150 hartree
zero-point correction: +0.418521 hartree
enthalpy correction: +0.442447 hartree
free energy correction: +0.365859 hartree
quasiharmonic free energy correction: +0.370032 hartree

TS11$_{endo1}$

C	4.31939	-0.99030	-0.54546
C	2.86502	-1.19678	-0.97216
C	1.85444	-0.74773	0.07837
C	2.39321	1.21008	0.30778
C	4.73610	0.46592	-0.36624
H	2.67471	-0.63085	-1.89495
H	4.48809	-1.52959	0.39998
H	4.96754	-1.45942	-1.29604
H	2.18617	1.41820	-0.74199
H	4.59073	0.98377	-1.32624
H	2.11036	-1.03195	1.09945
H	3.97684	0.65562	1.64724
H	4.21462	2.18763	0.80920
C	3.86093	1.15660	0.67555
C	0.49277	-0.82396	-0.27194
C	1.49079	1.69922	1.24998
H	1.82959	1.75310	2.28456
C	-0.45787	1.85878	-0.22671
C	0.13488	2.00285	1.00481
H	-0.48005	2.25797	1.86397
H	0.16435	1.68654	-1.10217
H	0.19737	-0.86081	-1.31521
C	6.20954	0.56435	0.02098
H	6.52558	1.60831	0.11732
H	6.84685	0.08394	-0.72839
H	6.38705	0.06827	0.98282
C	-0.52425	-0.93108	0.68436

O	-0.16509	-0.86494	1.97780
C	-1.88338	1.98862	-0.48089
C	-2.29110	1.83788	-1.76243
H	-1.51371	1.63847	-2.50105
C	-3.67698	1.89517	-2.31025
H	-3.75390	2.70792	-3.04244
H	-4.44439	2.04495	-1.54958
H	-3.89656	0.96875	-2.85560
C	-2.79860	2.24785	0.68582
H	-2.62403	1.52004	1.48605
H	-3.85069	2.19523	0.40299
H	-2.61187	3.24044	1.11171
C	2.63083	-2.68792	-1.26185
H	2.74671	-3.27746	-0.34504
H	1.62879	-2.86760	-1.65951
H	3.36396	-3.04725	-1.99120
C	-1.89689	-1.13620	0.39102
C	-2.54800	-1.27657	-0.86608
C	-2.90746	-1.15145	1.42691
N	-4.12400	-1.34554	0.86412
C	-4.04716	-1.34535	-0.58742
H	-4.54209	-0.46952	-1.02134
H	-4.47714	-2.24995	-1.02523
H	-4.97703	-1.17461	1.38050
O	-2.70536	-1.01532	2.66254
O	-2.08040	-1.36162	-2.01683
H	-0.99035	-0.90609	2.52854

SCF energy: –1097.679751 hartree
zero-point correction: +0.463916 hartree
enthalpy correction: +0.490157 hartree
free energy correction: +0.411088 hartree
quasiharmonic free energy correction: +0.413665 hartree
imaginary frequency: –419.7944

TS11$_{endo2}$

C	-4.32287	-0.88331	-1.06725
C	-2.89262	-0.57082	-1.53253
C	-1.83458	-0.90131	-0.48094
C	-2.48091	0.17969	1.10766
C	-4.84530	-0.13386	0.16142
H	-2.69384	-1.31070	-2.32217
H	-4.36299	-1.95767	-0.84245
H	-4.99981	-0.71439	-1.91361
H	-2.38880	1.11940	0.56542
H	-5.78834	-0.62200	0.43887
H	-1.99438	-1.86011	0.01141
H	-4.30247	0.21734	2.21450

H	-3.84818	-1.37878	1.62409
C	-3.89464	-0.31756	1.34664
C	-5.17509	1.34124	-0.08911
H	-5.70491	1.75930	0.77357
H	-5.82206	1.44989	-0.96609
H	-4.28470	1.95306	-0.25622
C	-0.49314	-0.58388	-0.78365
C	-1.53164	-0.06560	2.10065
H	-1.78013	-0.81336	2.85397
C	0.27122	1.31060	1.17543
C	-0.22593	0.46478	2.13867
H	0.44146	0.08629	2.90840
C	0.58446	-1.26062	-0.20188
H	-0.24968	0.16398	-1.52835
O	0.30460	-2.17685	0.74077
H	-0.40923	1.75641	0.45311
C	1.66112	1.72316	1.07304
C	1.97046	2.57923	0.07174
H	1.14756	2.89709	-0.56983
C	2.65453	1.14876	2.04756
H	2.45680	1.51002	3.06327
H	3.68111	1.41193	1.78916
H	2.58061	0.05591	2.07690
C	3.30341	3.13970	-0.29151
H	3.54166	2.87671	-1.33023
H	4.11302	2.79417	0.35276
H	3.27169	4.23488	-0.25188
C	1.94506	-1.06893	-0.55724
C	-2.70843	0.80723	-2.18103
H	-1.86218	0.80426	-2.87384
H	-3.60161	1.07555	-2.75359
H	-2.52972	1.60120	-1.44946
C	3.02516	-1.73612	0.13555
C	2.51252	-0.19914	-1.52957
N	4.20939	-1.36682	-0.41535
C	4.02887	-0.30971	-1.39754
H	4.47969	-0.55570	-2.36229
H	4.43756	0.64475	-1.04692
H	5.07755	-1.51467	0.08338
O	2.90800	-2.54711	1.09085
O	1.96983	0.52836	-2.38208
H	1.15919	-2.53336	1.09256

SCF energy: –1097.673513 hartree
zero-point correction: +0.465144 hartree
enthalpy correction: +0.491119 hartree
free energy correction: +0.412552 hartree
quasiharmonic free energy correction: +0.415227 hartree
imaginary frequency: –443.6348

TS11$_{exo1}$

C	-0.61838	2.27201	0.40278
C	0.49413	1.82368	-0.27046
C	-0.50257	-0.85075	0.42940
C	-1.84817	-0.83490	0.03322
C	-2.26507	0.94242	-0.90082
C	-1.93698	1.89532	0.05949
H	-0.48946	2.90773	1.27546
H	-2.73501	2.30211	0.67765
C	-2.92577	-0.94957	1.09892
H	-2.77135	-0.14694	1.83332
C	-3.70168	0.73805	-1.33613
H	-4.02637	1.62602	-1.89459
H	-3.74360	-0.10456	-2.03857
C	-4.67996	0.46501	-0.19002
C	-4.33923	-0.84752	0.51602
H	-4.47527	-1.67458	-0.19919
H	-5.05908	-1.01290	1.32726
H	0.35861	1.28820	-1.20813
H	-0.23486	-0.61266	1.45271
C	0.55324	-1.18619	-0.42778
O	0.26163	-1.44172	-1.71801
H	-2.07763	-1.35246	-0.90070
H	-1.52274	0.73540	-1.66926
H	-4.60927	1.28050	0.54256
C	-6.11231	0.42738	-0.71874
H	-6.38537	1.37602	-1.19220
H	-6.82476	0.23211	0.08925
H	-6.22481	-0.36745	-1.46606
C	1.86888	2.10509	0.08565
C	2.82084	1.68567	-0.78679
H	2.47108	1.17930	-1.68778
C	4.29788	1.88616	-0.70614
H	4.82183	0.96325	-0.98046
H	4.64102	2.21026	0.27769
H	4.60649	2.64154	-1.44006
C	2.15266	2.82961	1.37456
H	3.21862	2.85470	1.60369
H	1.63556	2.34626	2.20979
H	1.79254	3.86344	1.32559
C	1.90253	-1.26921	-0.02563
C	-2.77251	-2.29796	1.81699
H	-1.80188	-2.38029	2.31356
H	-2.86101	-3.12450	1.10231
H	-3.55827	-2.41537	2.57045
C	2.49070	-0.89463	1.22060
C	2.97613	-1.59102	-0.94331

N	4.15847	-1.59853	-0.26917
C	3.99827	-1.06666	1.07726
H	4.49385	-0.09724	1.19690
H	4.37610	-1.75311	1.83979
H	1.10470	-1.64906	-2.19256
H	5.02265	-1.47693	-0.78457
O	1.96199	-0.48699	2.26692
O	2.85544	-1.83895	-2.16817

SCF energy: –1097.679959 hartree
zero-point correction: +0.464101 hartree
enthalpy correction: +0.490400 hartree
free energy correction: +0.410744 hartree
quasiharmonic free energy correction: +0.413700 hartree
imaginary frequency: –406.4867

TS11$_{exo2}$

C	4.77520	-0.25968	-0.57508
C	3.71915	0.02941	-1.65616
C	2.32906	0.42647	-1.19118
C	1.80830	-1.10528	0.04973
C	4.31184	-1.37960	0.36427
H	1.53690	0.11479	-1.87022
H	3.61276	-0.87714	-2.26328
H	4.09809	0.81002	-2.32847
H	5.63253	-0.66695	-1.12686
H	1.90759	-1.79080	-0.79343
H	4.26841	-2.30768	-0.22129
C	0.49246	-0.91263	0.50783
H	0.30097	-0.46695	1.47602
C	2.09739	1.61020	-0.48990
H	2.94559	2.12975	-0.05317
C	0.81952	2.13942	-0.19890
H	0.77236	2.97072	0.50074
C	-0.35083	1.62466	-0.70554
H	-0.29806	0.88770	-1.50459
C	-0.63423	-1.31940	-0.21517
C	5.30976	0.97336	0.16334
H	5.58339	1.76206	-0.54622
H	6.20969	0.70172	0.72566
H	4.60176	1.39450	0.87898
O	-0.44699	-1.83668	-1.44570
C	2.94412	-1.22374	1.05306
H	2.76436	-2.20175	1.52600
H	5.07067	-1.53591	1.14102
C	-1.68390	2.07275	-0.36175
C	-2.70789	1.54572	-1.08007
H	-2.44162	0.83656	-1.86534

C	-1.84787	3.06657	0.75689
H	-2.89613	3.23218	1.00749
H	-1.40900	4.03326	0.48560
H	-1.33268	2.71861	1.65816
C	-4.16411	1.85587	-0.97514
H	-4.47970	2.43866	-1.84993
H	-4.42707	2.42001	-0.07908
H	-4.75256	0.93115	-0.99858
C	-1.95870	-1.22598	0.26512
C	2.88375	-0.19055	2.18077
H	2.03980	-0.39089	2.84776
H	3.79736	-0.23403	2.78170
H	2.77074	0.83023	1.80478
H	-1.33118	-2.07043	-1.82285
C	-2.44266	-0.57160	1.43738
C	-3.10467	-1.66750	-0.50095
C	-3.96330	-0.67733	1.41766
N	-4.23859	-1.47319	0.22895
H	-4.40329	0.32366	1.35044
H	-4.32127	-1.16067	2.33055
H	-5.12548	-1.39929	-0.25627
O	-1.82456	0.00694	2.34577
O	-3.08086	-2.16871	-1.65197

SCF energy: –1097.670615 hartree
zero-point correction: +0.465719 hartree
enthalpy correction: +0.491617 hartree
free energy correction: +0.413276 hartree
quasiharmonic free energy correction: +0.415783 hartree
imaginary frequency: –425.5739

3. Supporting References

1. Binninger, D. M.; Skrzynia, C.; Pukkila, P. J.; Casselton, L. A. *EMBO J*. **1987**, *6*, 835–840.
2. Johnson, M.; Zaretskaya, I.; Raytselis, Y.; Merezhuk, Y.; McGinnis, S.; Madden, T. L. *Nucleic Acids Res*. **2008**, *36*, W5.
3. Gottlieb, H. E.; Kotlyar, V.; Nudelman, A. *J. Org. Chem.* **1997***, 62*, 7512–7515
4. Nakazawa, T.; Ishiuchi, K.; Sato, M.; Mino, T.; Tsunematsu, Y.; Sugimoto, S.; Gotanda, Y.; Noguchi, H.; Hotta, K.; Watanabe, K. *J. Am. Chem. Soc*. **2013**, *135*, 13446–13455.
5. Tsunematsu, Y.; Ishikawa, N.; Wakana, D.; Goda, Y.; Noguchi, H.; Moriya, H.; Hotta, K.; Watanabe, K. *Nat. Chem. Biol*. **2013**, *9*, 818–825.
6. Tsunematsu, Y.; Ichinoseki, S.; Nakazawa, T.; Ishikawa, N.; Noguchi, H.; Hotta, K.; Watanabe, K. *J. Antibiot*. **2012**, *65*, 377–380.
7. Ishiuchi, K.; Nakazawa, T.; Ookuma, T.; Sugimoto, T.; Sato, M.; Tsunematsu, Y.; Ishikawa, N.; Noguchi, H.; Hotta, K.; Moriya, H.; Watanabe, K. *ChemBioChem* **2012**, *13*, 846–854.
8. Winter, J. M.; Sato, M.; Sugimoto, S.; Chiou, G.; Garg, N. K.; Tang, Y.; Watanabe, K. *J. Am. Chem. Soc.* **2012**, *134*, 17900–17903.
9. Sikorski, R. S.; Hieter, P. *Genetics* **1989**, *122*, 19–27.
10. Hélaine, V.; Rossi, J.; Gefflaut, T.; Alaux, S.; Bolte, J. *Adv. Synth. Catal*. **2001**, *343*, 692–697.
11. Yang, S. W.; Mierzwa, R.; Terracciano, J.; Patel, M.; Gullo, V.; Wagner, N.; Baroudy, B.; Puar, M.; Chan, T. M.; McPhail, A. T.; Chu, M. *J. Nat. Prod*. **2006**, *69*, 1025–1028.
12. Ishiuchi, K.; Nakazawa, T.; Yagishita, F.; Mino, T.; Noguchi, H.; Hotta, K.; Watanabe, K. *J. Am. Chem. Soc*. **2013**, *135*, 7371.
13. Qiao, K.; Chooi, Y. H.; Tang, Y. *Metab. Eng*. **2011**, *13*, 723.
14. Kakule, T. B.; Sardar, D.; Lin, Z.; Schmidt, E. W. *ACS Chem. Biol*. **2013**, *8*, 1549.
15. Jadulco, R. C.; Koch, M.; Kakule, T. B.; Schmidt, E. W.; Orendt, A.; He, H.; Janso, J. E.; Carter, G. T.; Larson, E. C.; Pond, C.; Matainaho T. K.; Barrows, L. R. *J. Nat. Prod*. **2014**, *77*, 2537–2544.

16. Sheldrick, G. M. *Acta Crystallogr. A.* **2008**, *64*, 112–122.

17. Gaussian 09, Revision D.01, Frisch, M. J.; Trucks, G. W.; Schlegel, H. B.; Scuseria, G. E.; Robb, M. A.; Cheeseman, J. R.; Scalmani, G.; Barone, V.; Mennucci, B.; Petersson, G. A.; Nakatsuji, H.; Caricato, M.; Li, X.; Hratchian, H. P.; Izmaylov, A. F.; Bloino, J.; Zheng, G.; Sonnenberg, J. L.; Hada, M.; Ehara, M.; Toyota, K.; Fukuda, R.; Hasegawa, J.; Ishida, M.; Nakajima, T.; Honda, Y.; Kitao, O.; Nakai, H.; Vreven, T.; Montgomery, J. A., Jr.; Peralta, J. E.; Ogliaro, F.; Bearpark, M.; Heyd, J. J.; Brothers, E.; Kudin, K. N.; Staroverov, V. N.; Kobayashi, R.; Normand, J.; Raghavachari, K.; Rendell, A.; Burant, J. C.; Iyengar, S. S.; Tomasi, J.; Cossi, M.; Rega, N.; Millam, M. J.; Klene, M.; Knox, J. E.; Cross, J. B.; Bakken, V.; Adamo, C.; Jaramillo, J.; Gomperts, R.; Stratmann, R. E.; Yazyev, O.; Austin, A. J.; Cammi, R.; Pomelli, C.; Ochterski, J. W.; Martin, R. L.; Morokuma, K.; Zakrzewski, V. G.; Voth, G. A.; Salvador, P.; Dannenberg, J. J.; Dapprich, S.; Daniels, A. D.; Farkas, Ö.; Foresman, J. B.; Ortiz, J. V.; Cioslowski, J.; Fox, D. J. Gaussian, Inc., Wallingford CT, 2013.

18. Zhao, Y.; Truhlar, D. G. *Theor. Chem. Acc.* **2008**, *120*, 215–241.

19. Marenich, A. V.; Cramer, C. J.; Truhlar, D. G. *J. Phys. Chem. B* **2009**, *113*, 6378–6396.

20. Zhao, Y.; Truhlar, D. G. *Phys. Chem. Chem. Phys.* **2008**, *10*, 2813–2818.

21. Ribeiro, R. F.; Marenich, A. V.; Cramer, C. J.; Truhlar, D. G. *J. Phys. Chem. B* **2011**, *115*, 14556–14562.

22. Avogadro: an open-source molecular builder and visualization tool. Version 1.1.1. http://avogadro.openmolecules.net/.

23. Hanwell, M. D.; Curtis, D. E.; Lonie, D. C.; Vandermeersch, T.; Zurek, E.; Hutchison, G. R. *J. Cheminform* **2012**, *4*, 17.

24. GaussView, Version 5, Dennington, R.; K., T.; Millam, J. Semichem Inc., Shawnee Mission KS, 2009.

25. CYLview, 1.0b; Legault, C. Y., Université de Sherbrooke, 2009 (http://www.cylview.org).

26. Schrödinger Release 2013-3: MacroModel, version 10.2, Schrödinger, LLC, New York, NY, 2013.

27. Schrödinger Release 2013-3: Maestro, version 9.6, Schrödinger, LLC, New York, NY, 2013.

28. Yamamoto, T.; Tsunematsu, Y.; Noguchi, H.; Hotta, K.; Watanabe, K. *Angew. Chem. Int. Eng. Ed.* **2015**, Submitted.